# Unique longitudinal contributions of sulcal interruptions to reading acquisition in children

Florence Bouhali [1,2, ✉], Jessica Dubois [3,4], Fumiko Hoeft [5] *, Kevin S. Weiner [6] *

*     co-senior authors

✉     corresponding author: florence.bouhali@gmail.com

1. Department of Psychiatry and Behavioral Sciences & Weil Institute of Neuroscience, University of California San Francisco, San Francisco, CA, USA.
2. Aix-Marseille University, CNRS, CRPN, Marseille, France.
3. University Paris Cité, NeuroDiderot, INSERM, Paris, France.
4. University Paris-Saclay, NeuroSpin, UNIACT, CEA, France.
5. Department of Psychological Sciences, University of Connecticut Waterbury, Waterbury, CT, USA.
6. Department of Psychology, Department of Neuroscience, Helen Wills Neuroscience Institute, University of California, Berkeley, Berkeley, CA, USA.

## Abstract

A growing body of literature indicates strong associations between indentations of the cerebral cortex (i.e., sulci) and individual differences in cognitive performance. Interruptions, or gaps, of sulci (historically known as *pli de passage*) are particularly intriguing as previous work suggests that these interruptions have a causal effect on cognitive development. Here, we tested how the presence and morphology of sulcal interruptions in the left posterior occipitotemporal sulcus (pOTS) longitudinally impact the development of a culturally-acquired skill: reading. Forty-three children were successfully followed from age 5 in kindergarten, at the onset of literacy instruction, to ages 7 and 8 with assessments of cognitive, pre-literacy, and literacy skills, as well as MRI anatomical scans at ages 5 and 8. Crucially, we demonstrate that the presence of a left pOTS gap at 5 years is a specific and robust longitudinal predictor of better future reading skills in children, with large observed benefits on reading behavior ranging from letter knowledge to reading comprehension. The effect of left pOTS interruptions on reading acquisition accumulated through time, and was larger than the impact of benchmark cognitive and familial predictors of reading ability and disability. Finally, we show that increased local U-fiber white matter connectivity associated with such sulcal interruptions possibly underlie these behavioral benefits, by providing a computational advantage. To our knowledge, this is the first quantitative evidence supporting a potential integrative gray-white matter mechanism underlying the cognitive benefits of macro-anatomical differences in sulcal morphology related to longitudinal improvements in a culturally-acquired skill.

## Introduction

Identifying neuroanatomical features associated with uniquely human cognitive abilities is a central goal in cognitive neuroscience. A growing number of empirical findings identify relationships between the morphology of indentations (known as sulci) in the cerebral cortex and individual differences in cognition (e.g., as reviewed in Cachia et al., 2021; Mangin et al., 2019; Weiner, 2019, 2023). For example, sulcal morphology in various human association cortices that have expanded significantly throughout evolution has been related to individual differences in abstract reasoning, executive function, inhibitory control, memory, face processing, and reading, as well as psychopathology (Amiez et al., 2018; Borst et al., 2014; Cachia et al., 2014; Garrison et al., 2015; Im et al., 2016; Lahutsina et al., 2023; Maboudian et al., 2024; Parker et al., 2023; Tissier et al., 2018; Voorhies et al., 2021; Willbrand et al., 2022; Yao et al., 2022). Moreover, recent research suggests that individual differences in sulcal interruptions are also related to individual differences in cognitive abilities such as numerical processing (Roell et al., 2021; Schwizer Ashkenazi et al., 2024), language and memory (Santacroce et al., 2024), and reading (Borst et al., 2016; Cachia et al., 2018). Sulcal interruptions (hereby referred to as *gyral gaps*) are a particular case of interconnecting gyri, historically known as *pli de passage* as coined by Gratiolet (1854), when they emerge on the brain surface. Nevertheless, it is presently unknown whether gyral gaps that are uniquely human are *longitudinally* (and thus likely causally) related to changes in cognitive abilities, especially in "evolutionarily new" domains such as reading.

For instance, previous work suggests that the maturation of a functional region for reading in ventral temporal cortex (hereafter VTC) when children learn to read, commonly referred to as the visual word form area (VWFA; Cohen et al., 2000; Dehaene et al., 2015; Dehaene & Cohen, 2011), is in part dependent on the pre-existing neural architecture of this region, in terms of both connectivity and cortical morphology (Beelen et al., 2019; Bouhali et al., 2014; Li et al., 2020; Moulton et al., 2019; Saygin et al., 2016; Skeide et al., 2016; Vandermosten et al., 2016). Of note, the human OTS is laterally displaced compared to the OTS in non-human primates (Natu et al., 2021). Additionally, recent studies have linked individual differences in the presence of gyral gaps in this laterally displaced human OTS to individual differences in reading skills (Borst et al., 2016; Cachia et al., 2018).

However, no study has yet explored if this unique neuroanatomical feature in human VTC is related to individual differences in reading skills, as well as other reading precursors (and related cognitive skills such as phonological awareness) as children learn to read - and additionally, if white matter changes may mediate this complex relationship.

Specifically, recent studies that identify relationships between sulcal morphology and cognition propose the novel hypothesis that this relationship reflects underlying differences in white matter architecture. Yet, to our knowledge, this hypothesis has not yet been tested. Sulcal interruptions are particularly interesting to study as they have been linked to a higher density of underlying short range white matter fibers (Bodin et al., 2021) - in which, mechanistically, a higher density of short range white matter fibers could provide a more efficient neuroanatomical infrastructure contributing to individual differences in human cognition compared to a less dense, and therefore, inefficient, neuroanatomical infrastructure. To test these options, here, we investigated whether the presence of left OTS interruptions serve as a longitudinal predictor of reading skills for the first time. We also examine the predictive power of these interruptions relative to benchmark cognitive precursors of reading and assess the role of white matter properties that may mediate this relationship.

Utilizing longitudinal data from 43 children followed from kindergarten at age 5 to age 8 on three measurement occasions, with comprehensive behavioral assessments of literacy, pre-literacy, cognitive skills, and MRI scans, our results provide novel evidence supporting that the interruption of the left posterior OTS (pOTS) is a robust longitudinal predictor of better reading skills, independent from—and more predictive than—typical pre-literacy skills. This relationship holds and accumulates across time, suggesting that the morphology of the left pOTS is a strong and consistent indicator of reading proficiency. Increased local U-fiber structural connectivity associated with left pOTS interruption may underpin the reading benefit of this neural marker. By exploring the neuroanatomical underpinnings of reading, our results highlight the intricate connection between the brain's evolved structure and its capacity to adapt to culturally invented cognitive demands, such as reading.

# Results

Due to previous findings showing (i) a link between gyral gaps of the occipito-temporal sulcus (OTS) and reading abilities (Borst et al., 2016; Cachia et al., 2018) and (ii) the importance of the neighboring mid-fusiform sulcus (MFS) as a cytoarchitectonic and functional landmark in VTC (Grill-Spector & Weiner, 2014; Weiner, 2019; Weiner et al., 2014), potentially relevant for graphemic orthographic processing (Bouhali et al., 2019), the OTS and MFS were delineated manually in each hemisphere, blindly from reading scores. This was done at each time point with available MRI scans (Time 1 at age 5 - T1, and Time 3 at age 8 - T3) on cortical surface reconstructions (in Freesurfer; Dale et al., 1999; Fischl et al., 1999; Reuter et al., 2012; Zaretskaya et al., 2018; see Materials and Methods) obtained by both cross-sectional and longitudinal pipelines (see Figure 1 for data overview and sulcal definitions, as well as Supplementary Figure 1 for a view of sulcal definitions in all participants). Because there were two $T_1$-weighted MRI scans per child (at T1 and T3), a within-subject template was created through the Freesurfer longitudinal pipeline to refine brain segmentations at each time point - an approach that increases the precision and discrimination of cortical surface reconstructions (Reuter et al., 2012). Brain-behavior relationships with regard to reading development described were restricted to the left pOTS, and other delineated sulci serve as controls to demonstrate its specificity.
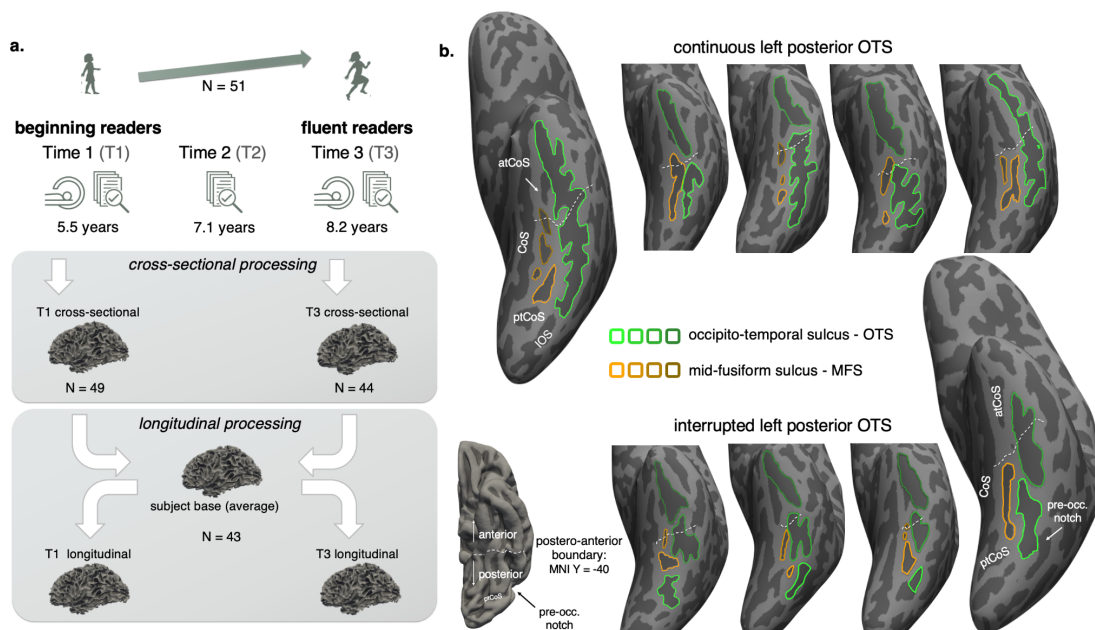


**Figure 1: Overview of the experimental design, analytical pipeline, and sulcal definitions. a.** Children were followed longitudinally from approximately 5.5 years of age (Time 1, T1) to age 8.2 (Time 3, T3) with both behavioral assessments and MRI scans, in addition to an intermediate behavior-only assessment at age 7.1 (Time 2, T2). $T_1$-weighted images from T1 and T3 were first processed separately in Freesurfer (cross-sectional processing), and then through the longitudinal pipeline with the creation of a subject template and refinement of T1 and T3 tissue segmentations. **b.** The occipito-temporal sulcus (OTS, green) and mid-fusiform sulcus (MFS, orange) were defined manually, as shown on 9 sample individual inflated left hemispheres (T1 longitudinal processing). Posterior and anterior sections of ventral temporal cortex were defined in each individual based on a boundary (dotted white line) located at MNI Y=-40 (see projection on Freesurfer average (*fsaverage*) surface on the bottom left, which roughly aligned with the anterior tip of the MFS). Left hemispheric views from exemplar children with continuous and interrupted left posterior OTS are shown on the top and bottom, respectively. CoS: collateral sulcus; ptCoS/atCoS: posterior/anterior transverse branch of the CoS; IOS: inferior occipital sulcus.

## When present, a gyral gap in the posterior OTS is a reliable longitudinal landmark

The OTS showed a very high incidence of interruption as a whole: approximately 79.3% of children showed at least one interruption in the left OTS, while 74.6% showed interruptions in the right OTS (see Supplementary Figure 2 for interruption statistics for all sulci, time points and processing pipelines). The posterior section of the OTS, whose interruption pattern has been more specifically implicated with

reading skills (Cachia et al., 2018), had at least one interruption in the left hemisphere in 56.5% of children, and in 58.3% in the right.

We further evaluated the stability and reliability of left pOTS interruption measurements across T1 and T3. Acceptable internal consistency in measuring the presence of left pOTS interruptions between T1 and T3 was observed when using segmentations from the cross-sectional processing pipeline (T1-T3 Cronbach's α = .778, estimated 95% confidence interval based on the procedure by Feldt et al. (1987): CI= [.591 - .880]). However, consistency was excellent and significantly improved with the longitudinal processing pipeline (T1-T3 α = .976, CI= [.958 - .976]). Visual inspection of participants with inconsistencies in measurements between T1 and T3 confirmed that these inconsistencies were due to noise in the $T_1$-weighted images at one time point and sub-optimal parcellations, rather than changes in anatomy *per se* across time points. Similarly, other anatomical measures, including sulcal length, sulcal interruption distance, surface area and thickness, also showed higher consistency using Freesurfer's longitudinal pipeline (see Supplementary Table 1 for the left pOTS). Left pOTS interruptions therefore appeared as a stable anatomical feature in time (at least in the 5- to 8-year-old range), in agreement with the prevailing view that the sulcal morphology of secondary sulci - including interruption patterns - is set in utero (Cachia et al., 2021). Left pOTS interruption was best measured with two $T_1$-weighted scans using Freesurfer's longitudinal (rather than cross-sectional) processing.

Because our interest lies in how sulcal morphology prospectively predicts the emergence of reading skills over time, we hereafter report the association between reading skills and left pOTS interruption measured through the longitudinal pipeline at Time 1 (T1). We report results from all 43 children who could be processed through this longitudinal pipeline (see participants' characteristics in Table 1). However, similar results are observed regardless of type of processing (longitudinal vs. cross-sectional) and time point used for the analyses (see Supplementary Information).

## Left pOTS interruption is prospectively associated with better reading skills

The presence of interruptions in the left pOTS at T1, measured with the longitudinal processing pipeline, was significantly associated with reading skills measured at T3. Compared with children with a continuous pOTS, children with an interrupted left pOTS at T1 showed higher reading TOWRE composite standard scores at T3, while controlling for demographic variables and total brain volume (see Figure 2a; F-test comparing nested models predicting TOWRE scores by age at T3, handedness and gender only, or by adding the residuals of a logistic regression explaining left pOTS interruption by total brain volume, age at T1, gender and handedness: $F(1,38)=11.34$, $p=1.7*10^{-3}$, $\Delta R^2=20.5\%$). This corresponded to a large effect size (Cohen's d on reading residuals accounting for demographic variables:  d = 0.957).

The association between left pOTS interruption and reading skills was robust to different measurements of reading skills and sulcal interruption in five ways. First, left pOTS interruption (measured at T1 with longitudinal processing) was predictive of reading skills as measured by all reading tests at T3, with a range of $\Delta R^2=13.4\%$ to 24.3% of variance explained on a variety of reading tests, ranging from accuracy and speed/fluency reading aloud single words and pseudo-words, to silent sentence reading and passage comprehension, as well as spelling scores (see Figure 2b). All of these associations were statistically significant ($p<0.012$). Interruption of the left pOTS was most strongly associated with passage comprehension and sentence reading scores.

Second, left pOTS interruption predicted T3 TOWRE composite scores regardless of whether it was measured through the longitudinal or cross-sectional processing pipeline of Freesurfer, at T1 or T3 (see Supplementary Figure 3a; T3 longitudinal: $F(1,38)=9.57$, $p=3.7*10^{-3}$, $\Delta R^2=17.9\%$; T1 cross-sectional: $F(1,40)=10.96$, $p=2.0*10^{-3}$, $\Delta R^2=19.6\%$; T3 cross-sectional: $F(1,39)=3.20$, $p=.08$, $\Delta R^2=6.62\%$), although the contribution was marginal at T3 with the cross-sectional pipeline. Third, despite more accurate tissue segmentations and better identification of left pOTS interruptions with longitudinal processing (see also Reuter et al., 2012), left pOTS morphology at T1 remained a significant longitudinal predictor of T3 reading without taking into account brain information at T3, i.e., with T1 cross-sectional processing alone. Fourth, associations between sulcal interruption and reading skills were specific to the left pOTS within VTC. No significant associations were observed for anterior OTS (aOTS) or MFS in either

hemispheres, or for the right pOTS (see Figure 2c, all p-values > 0.58, all $\Delta R^2$ < 0.7%).

Fifth, we tested whether interruption distance, as a continuous measure of sulcal interruption rather than the binary presence or absence of a gyral gap, was more predictive of reading skills. The total interruption distance between segments of the left pOTS was marginally predictive of future reading skills ($F_{(1,38)}$=3.54, p=.067, $\Delta R^2$=7.6%, see Supplementary Figure 3b). However, two additional analyses suggest that this association is likely due to trivial correlations between interruption distance and the binary presence of an interruption: (i) a similar analysis restricted to the subsample of children with interrupted left pOTS showed no association between reading and left pOTS total interruption distance ($F_{(1,21)}$<0.001, $\Delta R^2$=0.3%, p=.98); and (ii) interruption distance does not explain additional variance over and above the binary presence of an interruption across all children ($F_{(1,37)}$=0.04, p=.85), while binary interruption significantly explains more variance in reading skills over and above interruption distance ($F_{(1,37)}$=6.99, p=.012).

We further tested other anatomical features of the left pOTS at T1 and found that no other feature considered predicted reading skills, including total sulcal length, sulcal depth, depth of the sulcal pit, mean thickness, and total surface area (see Supplementary Figure 3b, all p-values > .26). In sum, the prospective relationship between left pOTS morphology at T1 and reading skills at T3 was specific to the binary presence of a gyral gap.
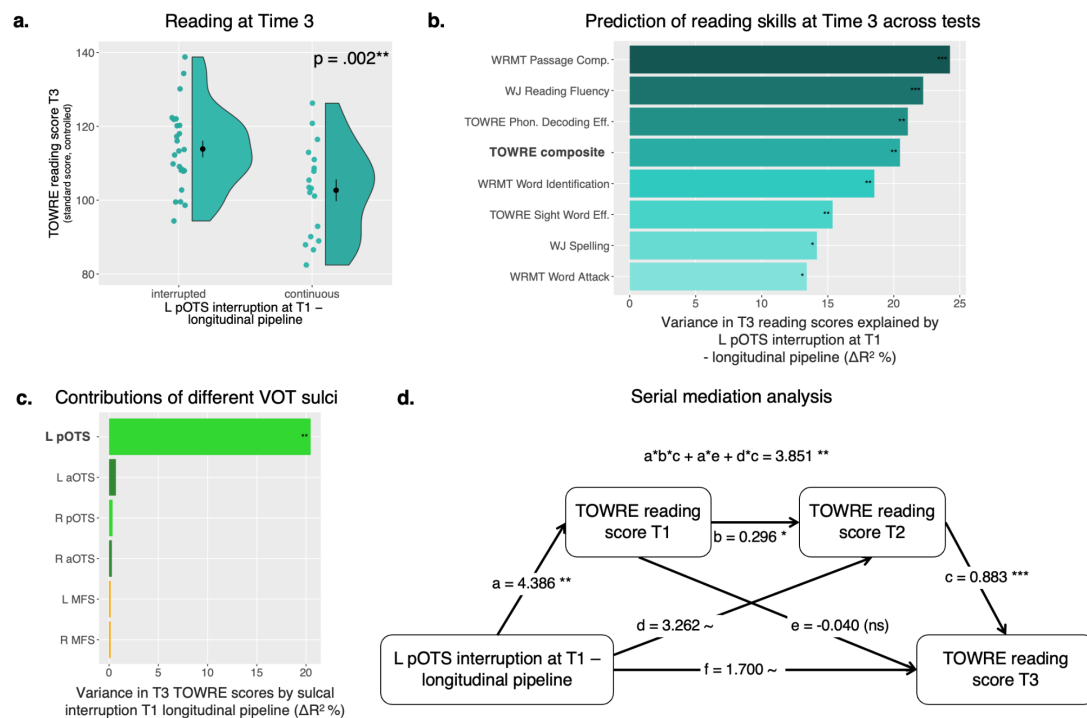


**Figure 2: Cumulative impact of left pOTS interruption on reading scores longitudinally. a.** TOWRE composite standard scores at T3 are significantly higher in children with an interrupted than continuous left pOTS (assessed at T1 with longitudinal processing), after removing residual variance due to age, gender and handedness. Black dots represent mean scores in each group, ± standard error of the mean (s.e.m.). **b. Prediction of reading and spelling scores across tests:** percentage of variance in different reading and spelling standardized tests explained by left pOTS interruption ($\Delta R^2$ in models controlling for demographic variables and total brain volume). Left pOTS interruption at T1 was significantly associated with all reading scores at T3, ranging from timed and untimed measures of single word and pseudo-word reading, as well as sentence and passage comprehension or spelling. The bolded TOWRE composite score corresponds to the effect depicted in panel a. **c. Percentages of variance in TOWRE T3 reading scores** explained by interruption by different sulci in VTC (posterior and anterior OTS (pOTS and aOTS, respectively) and MFS, in each hemisphere). **d. Serial mediation model demonstrating the cumulative impact of left pOTS interruption on TOWRE reading scores over time** from T1 to T2 to T3. Coefficients are standardized. Reading scores are controlled for age at testing, gender, and handedness, as well as left pOTS interruption by these demographic variables and total brain volume (***: p<0.001; **: p<.01, *: p<.05).

## The effect of left pOTS interruption on reading accumulates over time

We next tested whether the effect of left pOTS interruption on reading scores observed at T3 was present at earlier time points and how it evolved over time. Compared with children with a continuous left pOTS, children with interrupted left pOTS also had higher TOWRE composite reading scores at T2, at around 7.1 years-old, and already at T1, at approximately 5.5 years-old (see Supplementary Figure 4b and 4c; T2 TOWRE composite scores: $F_{(1,38)}=9.43$, $p=3.9*10^{-3}$, $\Delta R^2=14.3\%$, Cohen's d = 0.872; population-normalized T1 TOWRE composite scores, in the absence of norms in this age-range: $F_{(1,38)}=7.63$, $p=8.8*10^{-3}$, $\Delta R^2=16.0\%$, Cohen's d = 0.919).

However, differences in emerging reading skills at T1 did not alone drive the later differences observed at T2 and T3. Thus, a supplementary analysis on a subset of 24 children with lowest reading scores at T1 (i.e., with TOWRE T1 population-derived composite score equivalent < 95, hereafter referred to as *initial pre-readers*, see Methods) demonstrated that, although these children showed no difference in T1 reading scores depending on whether their left pOTS was interrupted or not ($F_{(1,19)}=0.21$, p =.66, $\Delta R^2=0.82\%$, Cohen's d = 0.034), there were growing statistically significant differences at T2 ($F_{(1,19)}=5.20$, p =.034, $\Delta R^2=16.91\%$, Cohen's d = 0.965) and at T3 ($F_{(1,19)}=6.93$, p =.016, $\Delta R^2=26.15\%$, Cohen's d = 1.107; see Supplementary Figure 4d-f).

A serial mediation analysis confirmed that the beneficial effect of left pOTS interruption on reading acquisition accumulated over time, from T1 to T2 and T3 (see Figure 2c). Residuals of T1, T2 and T3 TOWRE reading scores, controlled for age, gender and handedness, and residuals of a logistic regression of left pOTS interruption, accounting for demographic variables and total brain volume, were entered into a serial mediation model. T1 and T2 reading scores were significant serial mediators of the effect of left pOTS interruption on T3 reading, with left pOTS interruption at T1 predicting T1 TOWRE score (path a: estimated coefficient $\beta$= 4.386, standard error SE=1.560, p=.005), T1 TOWRE predicting T2 TOWRE (b: $\beta$=0.296, SE= 0.149 , p=.047) and T2 TOWRE predicting in turn T3 TOWRE (c: $\beta$=0.883, SE=0.104, p<.001). In addition to the indirect effect onto T3 TOWRE through T1 and T2 TOWRE scores, left pOTS interruption had marginal direct effects onto T2 TOWRE scores (d: $\beta$= 3.262, SE= 1.673, p=.051) and onto T3 TOWRE (f: $\beta$= 1.700, SE= 0.983, p=.08), suggesting that left pOTS interruption was a continued constraint on reading acquisition between 5 and 8 years of age. T2 TOWRE almost fully mediated the effect of T1 TOWRE reading onto T3 TOWRE (as shown by a non-significant direct path from T1 to T3 TOWRE, e: $\beta$=-0.040, SE=0.126, p=.75). The total serial mediation effect from left pOTS interruption to T3 TOWRE through T1 and T2 scores was significant (a*b*c + a*e + d*c: $\beta$=3.851, SE=1.450, p=.008).

## Left pOTS interruption is a stronger predictor of reading acquisition than pre-literacy skills

Having observed that left pOTS interruption before or at the onset of literacy acquisition is a strong predictor of future reading skills, we next asked how predictive this neuroanatomical feature was relative to benchmark cognitive predictors of reading skills, and how these variables related to one another. Specifically, we asked whether left pOTS interruption was a predictor of reading independent from known pre-literacy skills, or whether an association with a specific pre-literacy skill before learning to read may trivially explain its predictive power. We considered constructs shown to predict reading acquisition or risk of dyslexia longitudinally, as measured by classical neuropsychological tests: rapid naming (of colors and objects, as categories independent from early reading skills), phonological awareness, performance IQ, and receptive vocabulary. Letter knowledge and TOWRE scores at T1 were also considered, as emerging reading skills. Family history of dyslexia was also taken into consideration, and indexed by mother scores in the Adult Reading History Questionnaire (ARHQ, Lefly & Pennington, 2000, see Methods for reasons for selecting mother ARHQ).

Relative to all these predictors, left pOTS interruption was the strongest longitudinal predictor of reading, with its 20.5% of variance in T3 TOWRE explained after controlling for demographic variables ($\Delta R^2$, $F_{(1,38)}=11.34$, $p=1.7*10^{-3}$), followed by letter knowledge with 19.6% of variance (letter identification, $F_{(1,38)}=10.75$, $p=2.2*10^{-3}$) and phonological awareness with 16.2% (CTOPP, $F_{(1,38)}=8.51$, $p=5.9*10^{-3}$; see Figure 3a). Rapid naming (RAN objects and colors), early reading scores (TOWRE T1), family history

of dyslexia (mother ARHQ) and receptive vocabulary were also significant but weaker predictors of T3 reading skills, with separate respective contributions to T3 TOWRE scores of 13.6%, 11.5%, 11.2% and 9.5% of variance ($p \in [0.01, 0.04]$).

Concerning the extent to which left pOTS interruption is related at T1 to other longitudinal predictors of reading, we observed significant associations between sulcal interruption and early reading skills as previously reported, with left pOTS interruption accounting for $\Delta R^2 = 16.0\%$ in T1 TOWRE scores above demographic variables and total brain volume ($F(1,38)=7.63$, $p=8.8*10^{-3}$; see Figure 3b). We also observed significant contributions for explaining letter knowledge ($\Delta R^2 = 11.6\%$, $F(1,38)=6.09$, $p=.018$) and performance IQ (concept formation: $\Delta R^2 = 14.3\%$, $F(1,38)=6.78$, $p=.013$), but not for other variables ($p>.08$). A supplementary analysis on the subsample of 24 initial pre-readers at T1, i.e. removing confounds with early reading skills, still showed a potential association between left pOTS interruption and performance IQ ($\Delta R^2 = 14.2\%$, $F(1,19)=3.42$, $p=0.0797$, of marginal significance likely due to the reduced sample size given the effect size similar to that observed in the full sample), but no significant association with other pre-literacy skills (Figure S5g). Thus, the association between left pOTS interruption and performance IQ at T1 is reliable in our sample and independent from early reading skills, while the association with letter knowledge and TOWRE scores at T1 may only reflect early effects of left pOTS interruption on emerging reading skills.

Significant associations between left pOTS interruption, performance IQ and pre-literacy skills (Figure 3b), as well as potential associations between pre-literacy skills themselves (see Figure S5d and h), make it challenging to fairly assess the separate unique contributions of each of these variables to the longitudinal prediction of reading skills. Yet, when (over-)controlling for all pre-literacy skills and early reading abilities, as well as dyslexia family history, left pOTS interruption still had a marginal contribution to predicting T3 TOWRE reading scores ($\Delta R^2 = 5.0\%$, $F(1,31)=3.74$, $p=.062$), placing this sulcal measure as the third independent predictor of reading, after rapid naming and family history ($\Delta R^2=7.7\%$ and 6.6% for RAN and mother ARHQ respectively, see Figure S5b). When the same analysis was run in the subsample of initial pre-readers, to remove confounds between pOTS interruption and early reading skills, left pOTS interruption significantly contributed to predicting future T3 reading over and above all pre-literacy skills and family history ($\Delta R^2 = 27.8\%$, $F(1,12)=13.80$, $p=.003$), making it the first longitudinal contributor of reading, followed by performance IQ ($\Delta R^2 = 12.8\%$, $F(1,12)=6.34$, $p=.027$, Figure S5f).

In summary, left pOTS interruption at around 5 years of age stood out as the strongest longitudinal predictor of future reading skills at around 8 years, relatively to classical cognitive and familial predictors of reading ability and disability (dyslexia).
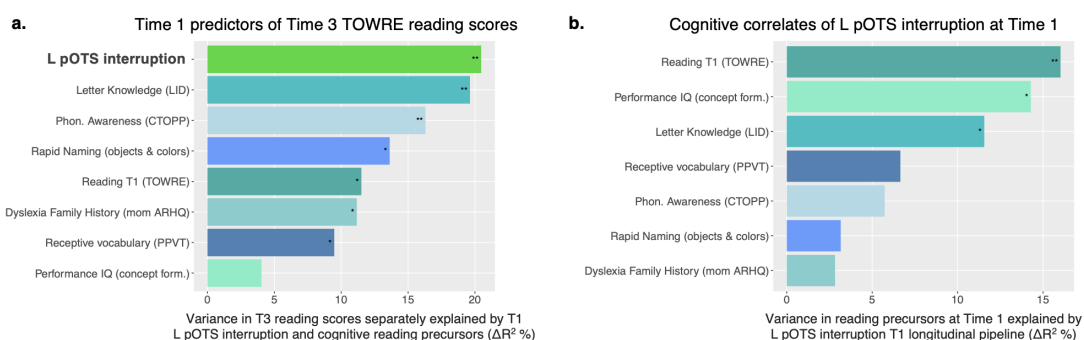


**Figure 3: Longitudinal contributions of left pOTS interruption to reading relative to cognitive precursors of reading, as well as their associations. a.** Variance in TOWRE reading scores at Time 3 explained by left pOTS interruption and classical predictors of reading at Time 1 separately, over and above demographic variables, ranked by decreasing contributions ($\Delta R^2$ in percentage). **b.** Associations between left pOTS interruption and predictors of reading at Time 1: percentage of variance ($\Delta R^2$) in left pOTS interruption explained by each pre-literacy skill separately, over and above demographic variables and total brain volume. (Stars on each bar denote significant contributions as assessed by nested model comparison using an F-test. **: $p<0.01$, *: $p<.05$)

## Why are interruptions beneficial? Left pOTS interruption and local white-matter connectivity advantages

The underlying mechanisms contributing to why the interruption in the cortical folds around the left pOTS region may so strongly and reliably favor adequate reading acquisition remains unknown. Previous work investigating the relationship between sulcal morphology and behavior have proposed a mediating role of the underlying white matter (Amiez et al., 2018; Borst et al., 2016; Cachia et al., 2018; Garrison et al., 2015; Miller et al., 2021; Voorhies et al., 2021), although these potential mechanisms have not been explicitly explored.

In the case of sulcal interruptions, two explanations stand out as potential mechanisms underlying the behavioral benefits for reading of left pOTS interruptions. First, given that white-matter fibers in general, and especially long-distance projection fibers, tend to terminate more in gyri than sulci (Dannhoff et al., 2023; Ge et al., 2018), having an extra gyral crown, or superficial *pli de passage* (Mangin et al., 2019), in the left pOTS may allow to pack more connections, especially long-distance connections through e.g., potentially a combination of fibers from the (posterior) arcuate fasciculus, vertical occipital fasciculus and inferior longitudinal fasciculus (Bouhali et al., 2014; Grotheer et al., 2021; Moulton et al., 2019; Weiner et al., 2017; Yeatman et al., 2012). Such increased long-distance connections may support a more efficient reading network. Alternatively, the presence of a *pli de passage* in the left pOTS may allow for better local white-matter connectivity through short-range U-shaped fibers traveling under the cortical gray matter. Indeed, Bodin and colleagues (2021) showed that, in the case of the superior temporal sulcus (STS), the presence of *plis de passage* was associated with a higher density of U-shaped fibers connecting adjacent gyri, with superficial *plis de passage* (i.e., sulcal interruptions with a full superficial gyral crown) showing an even higher local connectivity advantage than deep *plis de passage* (buried gyral gaps).

In order to test these hypotheses, we leveraged diffusion-weighted data available from Time 3 (n=29 children with data of sufficient quality, see Methods; too few children having usable diffusion data at T1). Gyral gaps between left pOTS sulcal components were manually delineated at the level of left pOTS interruption (see Figure 4a, and Supplementary Figure 6) and we assessed white-matter properties and connectivity around left pOTS gaps vs. left pOTS sulcal components (what we refer to as pOTS proper) in the same individuals (two leftmost violin plots in Figure 4b, top) and then also between individuals (individuals with uninterrupted pOTS and pOTS proper in individuals with an interrupted pOTS; right two violin plots in Figure 4b, top).

According to hypothesis (i), left pOTS gaps should show higher myelination, both in the cortex and the white-matter in its vicinity, than surrounding left pOTS components in the same individuals. Diffusion tensor models were therefore fitted to derive indices related to myelin content. Average Mean Diffusivity (MD) was first estimated in the cortical ribbon as the most robust DTI index reflective of myelination and neurite properties in the cortex (Fukutomi et al., 2019). In children with interruptions (n=15), MD in left pOTS gaps was higher than in the cortex of the left pOTS proper (paired two-sample T-test $t(14)=9.81$, $p=1.2*10^{-7}$ ; see Figure 4b, top row), while MD in the left pOTS proper of these children was similar to MD in the continuous left pOTS of the remaining children (n=14,Welch two-sample T-test: $t(25.6)=-0.39$, $p=.70$; Figure 4b top row, right handside). These results thus suggest lower myelination around left pOTS gaps, instead of the higher myelination predicted by hypothesis (i). This led to higher MD in the overall left pOTS in children with interruption - considering the cortex of the left pOTS proper and gyral gap(s) - than in children with continuous sulci ($t(26.4)=-2.18$, $p=.039$, Figure 4b bottom row). Additional analyses suggested that such differences were not driven by partial volume effects due to the presence of more or less surrounding white matter tissue or cerebro-spinal fluid close to gyral or sulcal cortex (see Supplementary DTI analyses in Supplementary Information).

The pattern of results observed for mean MD in the cortex was moreover confirmed by supplementary analyses of Radial Diffusivity (RD) and Fractional Anisotropy (FA) in the cortex around the left pOTS, and of MD, RD, and FA in the superficial white-matter located above the cortex (FA and RD being relevant markers of myelin content in white matter; see Dubois et al., 2014; Lazari & Lipp, 2021), suggesting higher myelination both in and above gyral gaps (Supplementary Figure 7). In short, against hypothesis

(i), the present data do not seem to support that left pOTS interruptions are associated with a connectivity advantage in terms of more terminations of long-distance projection fibers.
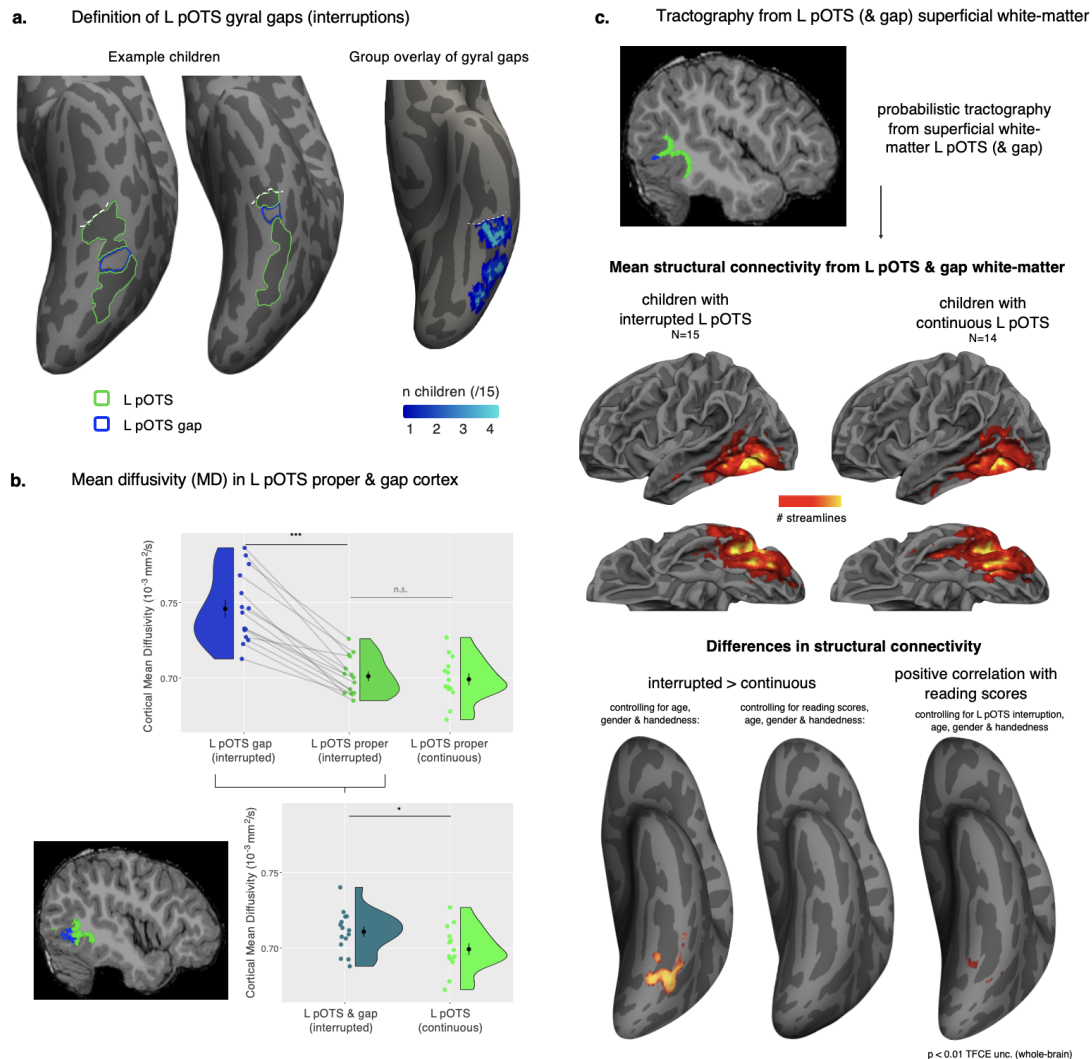


**Figure 4: White-matter correlates of left pOTS interruptions. a.** Gyral gaps in the left pOTS were delineated manually (in blue) and contrasted to left pOTS proper (green). Two exemplar left hemispheres are shown in children with a left pOTS interruption. The group-level map shows overlays of left pOTS gaps (projected onto the *fsaverage* surface) of 15 children with interrupted left pOTS, out of 29 with usable diffusion data. **b.** Average MD in the cortex of the left pOTS proper and gyral gaps. Top row (from left to right): difference in cortical MD in the left pOTS gap (blue) and left pOTS proper (dark green) in children with an interrupted sulcus, and in left pOTS in children with continuous sulci for comparison (light green). Bottom row, left: example cortical regions in which MD was average in a child with a sulcal interruption. Bottom row, right: MD comparison between children with interrupted and continuous sulci over the left pOTS cortex, including left pOTS gap if applicable. **c.** Probabilistic tractography from superficial white-matter seeds above the left pOTS cortex and possible left pOTS gap. From top to bottom: example seed in a participant (green: left pOTS proper, blue: left pOTS gap); mean whole-brain connectivity in children with interrupted (n=15) and continuous left pOTS (n=14); statistical differences in connectivity (from left to right): between the two groups not taking into account reading scores, between the two groups when modeling reading scores (no association observed), between connectivity and T3 TOWRE reading scores (p<0.01 TFCE uncorrected threshold).

Next, we tested hypothesis (ii) according to which left pOTS gaps would be associated with increased local connectivity surrounding the left pOTS, through the packing of more U-shaped fibers traveling superficially. In order to compare the structural connectivity around the left pOTS proper and gaps in children with a continuous vs. an interrupted sulcus, we performed whole-brain probabilistic tractography from a superficial white-matter layer located under the left pOTS and gap cortex (see Figure 4c for a seed region in an example participant). Mean structural connectivity from these seeds from all

children showed strong local connectivity to fusiform and inferior temporal gyri adjacent to the superficial white-matter seeds above the left pOTS, and extending to the middle temporal gyrus, parahippocampal cortex, and anterior OTS (Figure 4c middle panel), consistent with the presence of short, neighborhood association fibers traveling under the sulcal cortex (Dannhoff et al., 2023; Reveley et al., 2015). When comparing structural connectivity between children with interrupted and continuous left pOTS through permutation testing, children with sulcal interruption showed higher local connectivity, as indexed by density maps reflecting the number of reconstructed streamlines, in a cluster located around the posterior section of the left pOTS, after controlling for demographic variables (age, gender and handedness, p<0.01 threshold-free cluster enhancement -TFCE- uncorrected, Figure 4c bottom panel, leftmost map), suggesting a higher development of short-distance connections, in agreement with hypothesis (ii).

In order to assess whether this higher local connectivity in children with left pOTS gaps may also directly participate in their reading benefit, a second permutation analysis was run modeling the presence of left pOTS interruption, T3 TOWRE reading scores, and demographic covariates. In this analysis, no statistical difference was observed between children with and without interruptions (at p<0.01 TFCE), but connectivity and reading scores positively correlated in a white matter cluster that partially overlapped with the connectivity cluster from the previous analysis. Despite the reduced statistical power, this suggests that advantages in local structural connectivity around the posterior left pOTS in children with sulcal interruption may be associated with better reading scores and mediate the association between pOTS interruption and reading skills.

## Discussion

To the best of our knowledge, the current study provides empirical evidence for the first time supporting that the presence of a gyral gap of the left pOTS before, or at, the onset of literacy instruction robustly and uniquely predicts better future reading skills throughout the first three years of elementary school. Importantly, this effect was observed prospectively and was shown to accumulate over time. This marker of individual sulcal anatomy proved to be a large and independent contributor to shaping children's reading abilities, which outperformed predictions of reading skills based on well-established familial and pre-literacy cognitive measures. Increased local U-fiber connectivity around the left pOTS associated with the presence of a gyral gap appeared as a likely mechanism underlying the behavioral benefits of such gaps on reading development. Below, we discuss these results in the context of (i) robust and specific longitudinal associations between left pOTS interruptions and reading behavior, (ii) precision approaches to the study of the individual differences in cognition, (iii) developmental origins of the impact of left pOTS interruption on reading, and (iv) common processes by which cultural acquisitions rely on neuronal recycling.

### Robust and specific longitudinal associations between left pOTS interruptions and reading behavior

Previous findings demonstrated a cross-sectional association between left pOTS interruptions and reading ability in children (Borst et al., 2016) and adults (Cachia et al., 2018). Building on this work, the present findings showed a large positive contribution of left pOTS interruption to reading abilities in a population of beginning readers, and crucially, demonstrate its longitudinal validity: sulcal interruptions at the onset of literacy instruction in 5-6 year-olds predicted children's future reading skills at age 8.

Importantly, left pOTS interruptions were robustly associated with all aspects of reading tested at 8 years, ranging from single-word and pseudo-word naming (in both accuracy and speed), to sentence reading fluency and silent passage comprehension, as well as even spelling skills. Interestingly, the association between sulcal anatomy and reading was largest for passage comprehension - the most demanding and advanced aspect of reading.

Additionally, brain-behavior associations also extended to the most basic aspects of reading, e.g., letter recognition and orthographic processing, as demonstrated by significant associations between left

pOTS interruption and letter knowledge already at age 5, on top of associations with timed word and pseudo-word reading (Figure 3b). This *general* effect on reading skills thus extends beyond previous reports, established on reading measures mostly tapping into phonological decoding skills (Borst et al., 2016; Cachia et al., 2018). Moreover, left pOTS morphology may have an effect on reading development across alphabets throughout a wide range of orthographic depths, as we replicate in English prior results in French and Portuguese (Borst et al., 2016; Cachia et al., 2018) - two scripts much more transparent in terms of grapheme-to-phoneme conversion.

Interestingly, left pOTS interruption also showed associations with performance IQ at age 5 (see Figure 3b, and Supplementary Figure 5g), demonstrating additional associations with general cognitive skills. Though the interpretation of this domain-general association with cognition is unclear, the prospective association between left pOTS interruption and reading skills was not merely driven by such an association with general cognitive abilities at age 5 (Supplementary Figure 5b and f), consistent with our other results highlighting a high degree of specificity of left pOTS influences to reading abilities (e.g., no association with any other pre-literacy skill, Supplementary Figure 5c and g), and with the well-documented functional specificity of the left pOTS for orthographic processing and reading (e.g., Dehaene & Cohen, 2011; Gaillard et al., 2006; Pillet et al., 2024; Wilson et al., 2013; Zemmoura et al., 2015; Woolnough & Tandon, 2024; Zhan et al., 2023).

## Precision approaches to the study of individual differences in cognition

Results of the present study add to a growing body of literature indicating that inter-individual differences in the morphology of gyral gaps in association cortices are associated with various aspects of cognition such as numerical processing and reading skills (Borst et al., 2016; Cachia et al., 2018, 2021; Roell et al., 2021; Santacroce et al., 2024; Schwizer Ashkenazi et al., 2024; Tissier et al., 2018). The present and previous findings relating gyral gaps to individual differences in cognitive performance require manual definitions of gyral gaps in a relatively small sample of individuals, consistent with a "precision imaging" approach (Cachia et al., 2021; Gratton et al., 2022; Rosenberg & Finn, 2022). While brain-behavior relationships, typically studied through automatically-extracted estimates such as cortical thickness or surface area, have been found to have small effect sizes and to require large N approaches (Marek et al., 2022), macro-anatomical features of neuroanatomy may be expected to have a larger impact and require smaller samples. Moving forward, however, future studies can integrate these two approaches by building tools to precisely measure gyral gaps in an automated fashion, which would result in both a large N, as well as precisely identified gyral gaps, in each individual using deep learning (Lyu et al., 2021; Rivière et al., 2022).

## Developmental origins of the impact of left pOTS interruption on reading

Developmentally, the OTS starts to appear around 25-30 weeks of gestation (Chi et al., 1977; Garel et al., 2001; Hansen et al., 1993). Although the relative developmental timeline between the appearance of a sulcus and that of its interruptions remains unclear, interruption(s) of the OTS are thus thought to be stable features of neuroanatomy determined early on. In our study, we observed high reliability of the pOTS interruption from age 5 (T1) to age 8 (T3), which is consistent with the longitudinal stability of interruptions of (i) the intraparietal sulcus and postcentral sulcus (Schwizer Ashkenazi et al., 2024), (ii) sulci in inferior frontal cortex (Tissier et al., 2018), and (iii) patterns of the anterior cingulate sulcus (Cachia et al., 2016) observed in late childhood (approximately 8 years onwards) to early adulthood. Of course, genetic and environmental factors also likely contribute to the brain-behavior relationship identified in the present study. For example, a recent report has reported a marginal association in the interruption of the left OTS among mother-child dyads (Fehlbaum et al., 2022), suggesting potential contributions of genetic factors or of the familial environment in shaping left OTS morphology. Further, gyrification is significantly impacted by the prenatal environment (Amiez et al., 2018) and gestational age at birth (Dubois et al., 2019), notably in the case of regions surrounding the left pOTS (Papini et al., 2020; Schmitt et al., 2023). Multiple (e.g., twin) vs. single pregnancy and intrauterine growth restriction may also influence such gyrification patterns (Amiez et al., 2018; Dubois et al., 2008), each of which can be considered in future studies.

Moreover, in the present study, effects of left pOTS interruptions on reading skills accumulated and grew, as shown by significant serial mediation effects from T1 to T2 to T3 (Figure 2d). As such, left pOTS interruptions seem to have a continued beneficial influence on developing reading skills throughout the first few elementary grades. Whether such benefits to reading development continue to accumulate beyond 8 or 9 years of age remains to be explored, but these benefits seem to at least be retained later on, as suggested by reports in 10-year-olds (Borst et al., 2016) and adults (Cachia et al., 2018).

## Local connectivity differences at gyral gaps: Computational advantage?

The present findings empirically support that, despite variability in the location of individual gaps along the pOTS, children with at least one gyral gap have increased local connectivity in a posterior cluster of the left pOTS, compared to those with a continuous pOTS. Such increased connectivity could have a computational advantage. For instance, previous work has highlighted that junctions in gyral ridges, known as 3-hinge gyri, serve as hubs in cortico-cortical connections with higher connection degrees, stronger connections, and high betweenness centrality in graphs of structural connectivity (Zhang et al., 2020). The rich connectivity of such regions has also been documented through fine-grained post-mortem dissections (Shinohara et al., 2020; as also reviewed in Dannhoff et al., 2023), revealing that '*pyramid shape crossings*' are characterized by, and seem to result from, the convergence of both intra- and inter-gyral U fibers. Crucially, we showed that such increased local U-shaped fibers also relate to reading skills.

Building on these results, mechanistically, computational simulations of white-matter development and gyrification suggest that gyral regions with high concentration of growing axonal fibers tend to form 3-hinge gyri (Ge et al., 2018; see also Chavoshnejad et al., 2021). Therefore, pOTS gyral gaps may be intrinsically related to better U-fiber connectivity at the level where such gaps meet the adjacent fusiform and inferior temporal gyral crests. Such junctions may serve as connectivity hubs for processing written words, and such hubs may result in a computational advantage related to skilled reading, which can be tested in future research.

## Common processes, cultural acquisitions, and neuronal recycling

Interestingly, associations between sulcal interruptions and behavior have also been reported for symbolic, but not non-symbolic, number processing (Roell et al., 2021; Schwizer Ashkenazi et al., 2024), highlighting common processes by which cultural acquisitions relying on *neuronal recycling* (Dehaene & Cohen, 2007; Dehaene-Lambertz et al., 2018; Kubota et al., 2023) may be boosted by the presence pre-existing gyral gaps. In the case of the left pOTS, various other aspects of early brain structure have been proposed to constrain the development of reading skills and the neural network involved in reading such as: (i) anatomical connectivity (Bouhali et al., 2014; Grotheer et al., 2021; Li et al., 2020; Moulton et al., 2019; Saygin et al., 2016) and (ii) cortical morphology. In terms of the latter, a larger surface area of the left fusiform gyrus is associated with better reading outcomes in pre-reading children at familial risk of dyslexia (Beelen et al., 2019), and patterns of gray-matter volume around the VWFA longitudinally predict children that will become dyslexic (Skeide et al., 2016).

## Conclusion

Altogether, reading is a cultural invention too recent on the scale of human evolution to have influenced brain structure. Instead, the neural territories that become attuned for reading are said to be "*recycled*" for this evolutionarily new function when each child is taught how to read (Dehaene & Cohen, 2007; Dehaene-Lambertz et al., 2018; Kubota et al., 2023). Thus, it seems natural that structural properties of children's neural macro-architecture, such as the presence of left pOTS gyral gaps, may guide the neural plasticity during critical cultural learning experiences that may further impact learning outcomes. Our present findings support this hypothesis and link longitudinal measures of local cortical folding, white matter properties, and reading ability with a precision imaging approach for the first time.

## Materials and Methods

### Participants

51 children were followed longitudinally from kindergarten to third grade, as part of an NIH-funded project (K23HD054720) focusing on children's reading development. Specifically, children were assessed at three time points: T1 at a median age of 5.5 years, T2 at a median age of 7.1 years, and T3 around 8.2 years. Neuropsychological assessments, demographic and family information were collected at all time points, while only T1 and T3 included MRI acquisitions (see Figure 1a). Eight children were excluded from the main analyses assessing longitudinal associations between OTS and MFS morphology and reading acquisition: 4 children due to drop-out (did not come back for T3 visit), 1 due to neuroanatomical findings (large bilateral cysts in the anterior temporal lobe) and 3 due to excessive motion in the MRI at either T1 (2 children) or T3 (1 child). The resulting main sample consisted of N=43 children (58% males; 88% right-handed; see Table 1 for specific demographics). Children came from high socio-economic backgrounds (e.g., median average parental years of formal education: 17 years, equivalent to a master's degree) and had above-average cognitive abilities and reading skills, despite 42% of children having family history of dyslexia (e.g., a parent or sibling diagnosed with dyslexia, see Table 1). No child had received a diagnosis of dyslexia by T3, nor did any child qualify for such a diagnosis based on the in-depth neuropsychological assessments conducted in the study.

The Institutional Review Boards of Stanford University, where data were collected, and of the University of California San Francisco, where data were analyzed due to transition of the principal investigator FH, approved the present study. Informed assent and consent were obtained from children and their guardians, respectively. The dataset included in this study has resulted in several prior publications on other aspects of the data (Black et al., 2012; Hosseini et al., 2013; Myers et al., 2014; Vandermosten et al., 2020; Xia et al., 2021; Yamagata et al., 2016).

### Behavioral tests

Children were tested at T1, T2, and T3 with an extensive battery of standardized neuropsychological assessments concerning literacy and pre-literacy skills. Reading skills were assessed at all time points with the Sight Word Efficiency (SWE) and Phonemic Decoding Efficiency (PDE) sub-tests from the Test of Word Reading Efficiency (TOWRE first edition, Torgesen et al., 1999). In these tests, children had to correctly read aloud as many items as possible in 45 seconds from lists of increasing difficulty of high frequency words, often with irregular grapheme-phoneme mappings (sight words), and of pseudo-words (phonemic decoding). We used TOWRE scores as the primary measure of reading scores in the current study as this speeded reading score was most similar to speeded reading tests that had previously shown associations with the sulcation of the OTS (Borst et al., 2016; Cachia et al., 2018). At T1, letter knowledge was assessed through the Letter Identification sub-test of the Woodcock Reading Mastery Test R/NU (WRMT-R/NU, Woodcock, 1998). At T2 and T3, reading skills were also assessed with the Word Identification and Word Attack sub-tests from WRMT-R/NU, which respectively consist in untimed reading of low frequency words and of pseudo-words in isolation, with increasing difficulty. Additionally, the WRMT Passage Comprehension sub-test required children to appropriately complete a sentence or a short passage choosing a word among multiple options (pictures are included for a third of the easiest items). Reading Fluency and Spelling sub-tests from the Woodcock–Johnson III Tests of Cognitive Abilities (McGrew & Schrank, 2007) were also administered. In the Reading Fluency subtest, participants had to read a series of sentences and indicate for each whether it was true or false, within a 3-min time constraint. In the spelling subtest, children had to write down and correctly spell dictated words of increasing difficulty.

Children's cognitive and pre-literacy skills were also assessed, notably with the following tests: The Concept Formation sub-test of the WJ-III Tests of Achievement was used at T1 and T3 to estimate general cognitive abilities, and more specifically performance intelligence quotient (pIQ). Receptive vocabulary was measured with the Peabody Picture Vocabulary Test (fourth edition, Dunn & Dunn, 2007). Blending and Elision sub-tests from the Comprehensive Test of Phonological Processing (CTOPP first edition, Wagner et al., 1999) were used to derive a composite measure of phonological awareness. Rapid Automatized Naming (RAN) abilities were measured by averaging scores on the object and color sub-tests (Wolf & Denckla, 2005), to provide an estimate of rapid naming abilities independent from letter or symbol reading.

Information regarding family history of dyslexia was obtained using the Adult Reading History Questionnaire (ARHQ, Lefly & Pennington, 2000), for both parents (except for one father), and considering possible diagnosis of older siblings. Several measures of dyslexia family history were derived: a binary dyslexia family history variable (at least one parent or sibling with a dyslexia diagnosis, vs. none), mother and father ARHQ scores, as well as averaged parental ARHQ scores weighted by either total general or educational time spent with the child by each caregiver.

**Table 1: Sample demographics and main neuropsychological scores at the three time points T1-3** (median and inter-quartile range are indicated), for the N=43 children with longitudinal MRI processing.

| | |
|---|---|
| Gender | 18 Females / 25 Males |
| Handedness | 38 Right / 5 Left |
| Family history of dyslexia | 18 + / 25 - |
| Age T1 | 5.49 years [5.31 - 5.86] |
| Age T2 | 7.13 years [6.87 - 7.50] |
| Age T3 | 8.18 years [8.00 - 8.57] |
| TOWRE reading scores T1 | |
|   SWE (raw score) | 3.00 [0.00 - 9.00] |
|   PDE (raw score) | 2.00 [0.00 - 5.00] |
| TOWRE reading scores T2 | |
|   SWE (raw score) | 49.0 [38.0 - 58.5] |
|   PDE (raw score) | 18.0 [13.0 - 24.5] |
|   SWE (standard score) | 109.0 [103.0 - 120.0] |
|   PDE (standard score) | 104.0 [99.0 - 112.0] |
|   TOWRE composite (standard score) | 108.0 [101.0 - 118.0] |
| TOWRE reading scores T3 | |
|   SWE (raw score) | 61.0 [55.0 - 67.5] |
|   PDE (raw score) | 24.0 [20.0 - 35.5] |
|   SWE (standard score) | 110.0 [103.5 - 118.0] |
|   PDE (standard score) | 104.8 [98.0 - 115.0] |
|   TOWRE composite (standard score) | 108.9 [101.0 - 116.0] |
| Rapid Automatized Naming (standard score, average of color and object naming) | |
|   T1 | 98.0 [89.5 - 107.5] |
|   T2 | 97.0 [88.3 - 107.8] |
|   T3 | 97.0 [84.5 - 105.3] |
| Phonological awareness (CTOPP) (standard composite score of elision & blending subtests) | |
|   T1 | 112.0 [104.5 - 118.0] |
|   T2 | 118.0 [107.5 - 131.5] |
|   T3 | 119.8 [109.0 - 127.0] |
| Letter Knowledge T1 (WMRT) (standard score) | 110.0 [103.5 - 114.5] |
| Performance IQ (WJC Concept Formation, standard score) | |
|   T1 | 119.0 [106.0 - 127.0] |
|   T3 | 117.0 [109.0 - 123.0] |
| Socio-economic status | |
|   Average parental years of education | 17 years [16 - 18] |
|   Yearly household income (N=39) | 140k$ [88.5 - 200] |

## MRI Data acquisition

MRI data were acquired on a 3T GE Healthcare scanner at the Richard M. Lucas Center for Imaging at Stanford University using an eight-channel phased-array head coil. $T_1$-weighted ($T_1$w) images were acquired at T1 and T3 with a fast spoiled gradient echo sequence (repetition time: TR = 8.52 ms; echo time TE = 3.42 ms; inversion time TI = 400 ms; flip angle FA = 15 °; NEX = 1; 128 slices; thickness = 1.2 mm; field of view FOV = 22 cm; in-plane resolution = 256 × 256; voxel size = 0.859 × 0.859 × 1.2 mm).

Diffusion-weighted images (DWI) were collected with a high-angular resolution diffusion-imaging (HARDI) protocol at Time 3 with a single-shot spin-echo, echo-planar imaging sequence (46 axial 3mm-thick slices; repetition time TR = 5000 ms; echo time TE = 81.7 ms; in-plane resolution = 128 × 128; voxel size = 2.0 × 2.0 × 3.0 mm$^3$; 150 directions with b = 2500 s/mm$^2$; 6 volumes with b = 0 s/mm$^2$, posterior to anterior phase encoding). DWI data were successfully collected in 35 participants. Among these, one was excluded due to a neurological finding, 2 due to acquisition issues related to the bounding box

(missing parts of the brain) and 3 for excessive motion (see DWI processing), resulting in a final DWI sample at T3 of 29 children.

## $T_1$-weighted data processing

$T_1$-weighted images were processed in Freesurfer (Dale et al., 1999; Fischl et al., 1999) version 7.1.1, using the high-resolution sub-millimeter pipeline (Zaretskaya et al., 2018), in order to (1) segment gray and white matter, (2) reconstruct gray and white matter surfaces, and (3) dissociate sulcal from gyral components. Images were first processed cross-sectionally for each scan. When images were available at both Time 1 and Time 3 for a child (N=43), the longitudinal Freesurfer pipeline was used, which first creates an unbiased subject average across time points ("base") and then restarts multiple processing steps at each time point separately from the base template in order to refine tissue segmentations on each image (longitudinally processed images, Reuter et al., 2012; see Figure 1a). The application of such longitudinal processing steps has been demonstrated to result in more accurate assessments of anatomy and evaluation of longitudinal change, as we also confirmed.

Segmentations were inspected visually for quality of the acquisition and of the Freesurfer segmentation bilaterally in ventral occipito-temporal cortex susceptible to affect the identification of the OTS and MFS. This led to the rejection of 1 participant at T1 and 2 subjects at T3 due to excessive motion artifacts. An additional participant was excluded due to large bilateral arachnoid cysts in the anterior temporal lobe.

## Sulcal definitions & criteria

### Definition of the OTS and MFS

The OTS and MFS were identified manually, for each participant at each time point (T1 and T3), and processing pipeline (Freesurfer cross-sectional vs. longitudinal). Sulci were labeled by FB and verified or corrected by KW. Sulcal labeling was blind to the children's reading scores, and relied on the identification and the anatomy of nearby sulci based on previous criteria from our group (Weiner, 2019; Weiner et al., 2014) and others (Cachia et al., 2018). Surrounding sulci considered when defining the OTS and MFS included the collateral sulcus (CoS) medially, the posterior transverse collateral sulcus (ptCoS) posteriorly, the anterior transverse CoS (atCoS) anteriorly, and the inferior and superior temporal sulci (ITS and STS) laterally. Additionally, the pre-occipital notch (see Figure 1a) was referenced as a useful landmark identifying the posterior extent of the OTS on the pial surface. Sulci were defined on Freesurfer's inflated surface as components with negative curvature, taking into consideration folding patterns as seen in the volume or white and pial surfaces, and potentially exclusive of connected branches corresponding to other sulci.

The ptCoS was first identified as the sulcus extending from the CoS-proper (Petrides, 2019) and forming the posterior boundary of the fusiform gyrus.

The OTS was then defined as the long and deep sulcus separating the fusiform gyrus from the inferior temporal gyrus. As such, its posterior boundary was defined by a virtual line extending from the ptCoS to the pre-occipital notch (as best identified on the pial surface), which delineates the boundary between temporal and occipital cortex (Ono et al., 1990; Duvernoy et al., 1999; Petrides, 2019). Note that, as a consequence, our OTS definition is exclusive of occipital components and branches, considered as the inferior occipital sulcus, although we retained the classical denomination of the *occipito*-temporal sulcus. In cases when the OTS extended into occipital cortex, the OTS-proper was thus interrupted at the level of a *pli de passage* most consistent with the virtual line between the ptCoS and pre-occipital notch. The pre-occipital notch was not considered as part of the OTS and excluded from OTS delineations in the frequent case where it was connected to the OTS. Just as the ptCoS can be considered as the posterior hook identifying the posterior extent of the fusiform gyrus, the atCoS can be considered as an anterior hook identifying the anterior extent of the fusiform gyrus (Duvernoy et al., 1999). Laterally, the identification of the ITS, and of the STS and its posterior branches (Huntgeburth & Petrides, 2012), were used to disambiguate OTS components in complex cases.

The MFS was defined as the longitudinal sulcus that divides the fusiform gyrus into lateral and medial components following guidelines by Weiner and colleagues (Weiner et al., 2014; as also reviewed in Weiner, 2019). One characteristic feature of the MFS, due to its location in between the CoS and OTS on the cortical surface, is that it forms a distinct ω shape on coronal slices (corresponding to the middle bump of the ω). Indeed, as a putative tertiary sulcus, the MFS is about half as deep as the surrounding

OTS and CoS (Weiner et al., 2014). Additionally, the anterior tip of the MFS consistently aligns with the posterior tip of the hippocampus (Grill-Spector & Weiner, 2014).

### Posterior / anterior OTS

A fixed boundary in MNI template space at coordinate Y=-40 was used to distinguish posterior sections of the OTS (corresponding to typical coordinates of the VTC) from anterior sections. Posterior and anterior volumes in MNI space were first transformed to Freesurfer average subject space (*fsaverage*), then projected onto the *fsaverage* surface, and finally projected onto each individual surface, to split the OTS into posterior and anterior sections (pOTS and aOTS respectively, see Figure 1b).

### Definition of gyral gaps / plis de passage for T3 DWI analyses

In order to investigate white-matter properties of the sulcal interruptions that may be associated with a reading benefit, the gyral gaps, including gyral crowns, located between chunks of the left pOTS were delineated manually by outlining the nearest points between the sulcal components (as shown in Figure 4).

## Sulcal measurements

From the defined OTS, pOTS, aOTS, and MFS, seven anatomical features were extracted as possibly relevant features: (i) sulcal interruption, (ii) interruption distance between sulcal components, (iii) sulcal length, (iv) sulcal depth, (v) depth of the sulcal pit, (vi) sulcal thickness, and (vii) sulcal surface area. Interruption distance between sulcal components was considered as Cachia and colleagues (2018) observed an association between the size of left pOTS interruptions along the postero-anterior axis and reading skills. In the present work, interruption distance was measured as the Euclidean distance between two sulcal components, or the sum of distances in instances where there were three or more components of a sulcus. Specifically, following the procedure by Borst, Cachia and colleagues (Borst et al., 2016; Cachia et al., 2018), sulcal interruptions were counted as such when sulcal components were separated by at least 1mm, or when the total interruption distance across all components of a sulcus was larger than 1mm, as very small interruptions may be attributable to noisy scans or bad brain segmentations. Sulcal length was considered as a complementary feature of sulcal interruption and interruption distance, known to be behaviorally relevant (see e.g., Parker et al., 2023, for associations between MFS length and facial recognition abilities). Sulcal length was measured by custom software as the largest geodesic distance between any two points within a given sulcal component, or the sum of lengths of all sulcal components in cases of interrupted sulci. Sulcal depth was measured using the *calcSulc* toolbox (Madan, 2019), by extracting the median Euclidean distance of the 8% deepest vertices of a given sulcus (as identified by Freesurfer *sulc* values) to the enclosing brain surface. We chose to select the 8% deepest vertices, rather than the initially set number of vertices (100 in the toolbox), in order to prevent the biasing of sulcal depth across sulci of different sizes (notably the much smaller MFS). Results were unchanged when using a percentage of deepest vertices ranging from 4 to 12%. The depth of the sulcal pit was also considered as sulcal pits often constitute stable functional and behavioral landmarks (e.g., Natu et al., 2021).

## DWI processing

Each diffusion-weighted image was first denoised using the Marchenko-Pastur principal component analysis technique implemented in MRTrix3 (Veraart et al., 2016). Because no diffusion data with reverse phase encoding was available, distortions due to susceptibility artifacts were corrected using the *Synb0-DISCO* approach (Schilling et al., 2020). Accordingly, an undistorted b0 image was estimated using deep learning (3D U-nets) in order to match the geometry of structural $T_1$w images and intensity contrasts from diffusion images. The distortions were then estimated and applied using the *topup* tool in FSL (Andersson et al., 2003). Both distortion and motion corrections were applied using the *eddy* function in FSL (Andersson & Sotiropoulos, 2016). Due to relatively high motion in this pediatric sample, *eddy* was run with conservative options consisting in 8 iterations with decreasing amounts of smoothing at 10, 6, 4, 2, 0, 0, 0, 0 mm full width at half maximum (FWHM), with additional outlier detection and replacement, and estimation of susceptibility-induced field changes by subject movement (Andersson et al., 2018). Volumes with more than 10% of outlier slices as identified by *eddy*, or with more than 1 mm of

displacement relative to the previous volume, were excluded. Three participants with more than 10% of discarded volumes were excluded from further analyses, resulting in a final sample of 29 children with DWI data at Time 3.

In order to most accurately align individual $T_1$w and DWI data, non-linear transformations were estimated using Advanced Normalization Tools (ANTs, Avants et al., 2011) between the participant's bias-corrected $T_1$w image and the individual average of all distortion-corrected b0 images (which have a relatively high gray/white contrast compared to other DWI-derived images). Specifically, non-linear transformations were used as an additional measure to correct for distortions induced in VTC by susceptibility artifacts due to the proximity of air/tissue interfaces in the nearby ear canals.

DWI data were first used to derive diffusion tensor indices in order to compare microstructural properties of the cortex and white matter around the left pOTS between sulcal components per se and the gyral gaps, and between children with and without interruptions. Second, probabilistic tractography from this region was performed to investigate the correlates of pOTS interruptions in terms of structural connectivity, between groups of children and according to reading scores.

The tensor model was estimated in FSL using *dtifit* in order to derive diffusion-tensor imaging (DTI) maps of mean and radial diffusivities (MD and RD) and fractional anisotropy (FA), as indices of myelin content. While MD is the most robust DTI index reflective of myelination and neurite properties in the cortex (Fukutomi et al., 2019), FA and RD are relevant markers of myelin content in white matter (Dubois et al., 2014; Lazari & Lipp, 2021).
To estimate MD, RD, and FA values most accurately in the cortical ribbon and superficial white matter above the left pOTS and its interruptions, individual MD, RD, and FA maps were transformed into native $T_1$w space and averaged within local masks of the cortical ribbon and superficial white matter. These masks were obtained by propagating Freesurfer labels of the left pOTS and its interruptions into the volumes using the *mri_label2vol* function, either into the whole cortical ribbon or into a 2-voxel-thick layer of the superficial white matter (see Figure 4b and c). Additionally, a white matter mask was used to prevent the white-matter layer from extending into gray matter voxels of neighboring sulci.

To identify differences in structural connectivity associated with interruption of the left pOTS, probabilistic tractography was performed from a mask of superficial white matter located above the left pOTS labels, inclusive of the gyral crowns of the interruption(s) / *pli(s) de passage* in children with left pOTS interruption. Masks of superficial white matter above the left pOTS and interruptions were transformed from T1-w images into diffusion native spaces through ANTs using nearest-neighbor interpolation, to serve as tractography seeds. FSL's *bedpostx* function (Bayesian Estimation of Diffusion Parameters Obtained using Sampling Technique) was used to estimate distributions of diffusion parameters and to model crossing fibers in each voxel (3 fibers per voxel). *Probtrackx* was used to perform probabilistic tractography from individual seeds, using the Euler integration for the precise computing of probabilistic streamlines, distance correction to compensate for the fact that connectivity distribution drops with distance from the seed mask, and with segmentations of gray matter and ventricles as termination masks. The minimum allowable angle between two tractography steps was set to 30 degrees, to allow for the reconstruction of U-shaped fibers, which pass by the white-matter underlying sulcal fundi connecting adjacent gyri - in this case, the fusiform and inferior temporal gyri. Because seed volumes significantly differed between children with interrupted and continuous left pOTS, the number of streamlines started per seed voxel in the tractography algorithm was scaled individually based on seed volume to correspond to an average of 5,000 seeds per voxel (default value in *probtrackx*) and to yield similar total numbers of streamlines. The latter was implemented in order to accurately assess group differences in structural connectivity, unbiased by seed volume. Individual masks of gray matter and ventricles were used as stop masks for the tractography. Distance correction and modified Euler streamlining options were used to improve the accuracy of tractography. The obtained individual probabilistic fiber density maps were then transformed into template MNI space for statistical analysis using non-linear registration in ANTs, from individual diffusion space (individual FA map) to the HCP1065 MNI FA template, and smoothed with a 4-mm-FWHM Gaussian kernel. Voxel-wise permutation (non-parametric) testing was performed with FSL's *randomise* function (Winkler et al., 2014), to assess the effect of left pOTS interruption on structural connections of its underlying white-matter, controlling for

age, gender and handedness. Results of such permutation tests were compared to those of a similar model with reading scores (controlled for demographic variables) as an additional predictor, so as to assess whether differences in structural connectivity were more attributable to interruption of the left pOTS or differences in reading skills.

## Statistical analyses

Statistical analyses were performed in R version 4.2.2 (R Core Team, 2022). The impact of sulcal anatomical features on reading skills, or other test scores, across time points was assessed while controlling for the possible impact of demographic variables (e.g., age, gender and handedness, on top of total brain volume (TBV) in the case of sulcal features). Specifically, for each sulcal feature and each assessment score of interest, an F-test was performed to compare two nested models predicting scores at time $T_i$ (i=1, 2 or 3) from demographic variables only (baseline model), or taking into additional consideration sulcal features measured at time $T_j$ (j= 1 or 3), controlled for nuisance variables, (test model) as follows:

Baseline model:   $Score_{Ti} \sim Age_{Ti} + Gender + Handedness$
Test model:         $Score_{Ti} \sim Age_{Ti} + Gender + Handedness$
                        $+ residuals( logit(sulcal\ interruption_{Tj} \sim Age_{Tj} + TBV_{Tj} + Gender + Handedness))$

where *logit* indicates a logistic regression.
Or, in the case of continuous sulcal measurements:
Test model:         $Score_{Ti} \sim Age_{Ti} + Gender + Handedness$
                        $+ residuals(sulcal\ measure_{Tj} \sim Age_{Tj} + TBV_{Tj} + Gender + Handedness)$

F-statistics and associated p-values are reported for these nested model comparisons, as well as the difference in variance explained between models ($\Delta R^2$ in %). For more coherence with statistical tests, plotted scores are controlled for demographic variables (age, gender and handedness; i.e., residuals are plotted, after adding back population mean to retain the estimation of average scores, see e.g., Fig. 2a or Fig. S4). Plots were created using the R *ggplot2* package (Wickham, 2016). Early publicly available code corresponding to the R *ggrain* package was adjusted to create *raincloud plots* (Allen et al., 2019). To investigate the unique contributions of several predictors of reading (see for instance Figure S5b and f) while controlling for other variables, such predictors were added to both the baseline and test models, following the same logic. Finally, to investigate possible associations at T1 between sulcal interruption and precursors of reading, we compared the model fits between nested logistic regressions predicting left pOTS interruption based on demographic variables and TBV (baseline), including or not each reading precursor separately as follows:

Baseline model:   $logit(sulcal\ interruption_{T1} \sim Age_{T1} + TBV_{T1} + Gender + Handedness)$
Test model:         $logit(sulcal\ interruption_{T1} \sim Precursor\_score_{T1}$
                        $+ Age_{T1} + TBV_{T1} + Gender + Handedness)$

Statistics were conducted on standard scores from the standardized neuropsychological tests as they are more normally distributed than raw scores (a requirement for parametric tests). More importantly, the rationale of the study is to assess whether sulcal morphology will predict whether a child is going to be a relatively good reader or not, independently from age. Note that despite standardization of raw scores within age bins in some tests, age still had a residual significant effect on test scores (TOWRE T3 standard score notably) and was therefore included in baseline models. Because the TOWRE is not normed below 6 years of age, an equivalent of a composite TOWRE standard score was obtained for T1 by scaling the principal component of T1 SWE and PDE raw scores (to a mean of 100 with standard deviation of 15).

To reduce degrees of freedom concerning measures of dyslexia family history, a stepwise backward selection was applied to identify family history measure(s) that best predicted T3 TOWRE composite scores (accounting for age, gender and handedness). Binary family history factor (i.e. *does a direct relative have a formal diagnosis?*), mother and father ARHQ scores and their weighted averages based on educational and total general parental time spent with the child were entered into the model. Among

these, mom ARHQ scores were selected as the most reliable measure predicting children TOWRE T3 reading scores, without any significant additional contribution from other variables.

Because some children already knew how to read at Time 1 (median of 3 words read in 45s in the SWE subtest, ranging from 0 to 58; median of 2 syllables or pseudowords read in 45s in the PDE subtest, ranging from 0 to 36), complementary analyses were performed to (i) investigate whether the predictive power of left pOTS interruption held in a population of children who were pre-readers at T1 (Fig. S4), and (ii) to better assess the effect size of independent contributions of left pOTS morphology on future reading skills (Fig. S5) over initial reading scores at T1 (to which it was already correlated). We therefore selected a subsample of children whose TOWRE standard score equivalent at Time 1 was below 95, resulting in a subset of 24 *initial pre-readers* (median of 0 words read in 45s in SWE, range: 0-7; median of 0 syllables in 45s in PDE, range: 0-4).

The serial mediation analysis was performed using the R *lavaan* package (Rosseel, 2012). Parameter estimates and confidence intervals were estimated using 10,000 bootstrap samples.

## Acknowledgements

# References

Allen, M., Poggiali, D., Whitaker, K., Marshall, T. R., van Langen, J., & Kievit, R. A. (2019). Raincloud plots: A multi-platform tool for robust data visualization. *Wellcome Open Research*, *4*. https://www.ncbi.nlm.nih.gov/pmc/articles/PMC6480976/

Amiez, C., Wilson, C. R. E., & Procyk, E. (2018). Variations of cingulate sulcal organization and link with cognitive performance. *Scientific Reports*, *8*(1), 13988. https://doi.org/10.1038/s41598-018-32088-9

Andersson, J. L. R., Graham, M. S., Drobnjak, I., Zhang, H., & Campbell, J. (2018). Susceptibility-induced distortion that varies due to motion: Correction in diffusion MR without acquiring additional data. *NeuroImage*, *171*, 277–295. https://doi.org/10.1016/j.neuroimage.2017.12.040

Andersson, J. L. R., Skare, S., & Ashburner, J. (2003). How to correct susceptibility distortions in spin-echo echo-planar images: Application to diffusion tensor imaging. *NeuroImage*, *20*(2), 870–888. https://doi.org/10.1016/S1053-8119(03)00336-7

Andersson, J. L. R., & Sotiropoulos, S. N. (2016). An integrated approach to correction for off-resonance effects and subject movement in diffusion MR imaging. *NeuroImage*, *125*, 1063–1078. https://doi.org/10.1016/j.neuroimage.2015.10.019

Avants, B. B., Tustison, N. J., Song, G., Cook, P. A., Klein, A., & Gee, J. C. (2011). A reproducible evaluation of ANTs similarity metric performance in brain image registration. *NeuroImage*, *54*(3), 2033–2044. https://doi.org/10.1016/j.neuroimage.2010.09.025

Beelen, C., Vanderauwera, J., Wouters, J., Vandermosten, M., & Ghesquière, P. (2019). Atypical gray matter in children with dyslexia before the onset of reading instruction. *Cortex*, *121*, 399–413. https://doi.org/10.1016/j.cortex.2019.09.010

Black, J. M., Tanaka, H., Stanley, L., Nagamine, M., Zakerani, N., Thurston, A., Kesler, S., Hulme, C., Lyytinen, H., Glover, G. H., Serrone, C., Raman, M. M., Reiss, A. L., & Hoeft, F. (2012). Maternal history of reading difficulty is associated with reduced language-related gray matter in beginning readers. *NeuroImage*, *59*(3), 3021–3032. https://doi.org/10.1016/j.neuroimage.2011.10.024

Bodin, C., Pron, A., Le Mao, M., Régis, J., Belin, P., & Coulon, O. (2021). Plis de passage in the superior temporal sulcus: Morphology and local connectivity. *NeuroImage*, *225*(October 2020), 117513. https://doi.org/10.1016/j.neuroimage.2020.117513

Borst, G., Cachia, A., Tissier, C., Ahr, E., Simon, G., & Houdé, O. (2016). Early Cerebral Constraints on Reading Skills in School-Age Children: An MRI Study. *Mind, Brain, and Education*, *10*(1), 47–54. https://doi.org/10.1111/mbe.12098

Borst, G., Cachia, A., Vidal, J., Simon, G., Fischer, C., Pineau, A., Poirel, N., Mangin, J.-F., & Houdé, O. (2014). Folding of the anterior cingulate cortex partially explains inhibitory control during childhood: A longitudinal study. *Developmental Cognitive Neuroscience*, *9*, 126–135. https://doi.org/10.1016/j.dcn.2014.02.006

Bouhali, F., Bézagu, Z., Dehaene, S., & Cohen, L. (2019). A mesial-to-lateral dissociation for orthographic processing in the visual cortex. *Proceedings of the National Academy of Sciences*, *116*(43), 201904184. https://doi.org/10.1073/pnas.1904184116

Bouhali, F., de Schotten, M. T., Pinel, P., Poupon, C., Mangin, J.-F., Dehaene, S., & Cohen, L. (2014). Anatomical connections of the visual word form area. *Journal of Neuroscience*, *34*(46). https://doi.org/10.1523/JNEUROSCI.4918-13.2014

Cachia, A., Borst, G., Jardri, R., Raznahan, A., Murray, G. K., Mangin, J.-F., & Plaze, M. (2021). Towards Deciphering the Fetal Foundation of Normal Cognition and Cognitive Symptoms From Sulcation of the Cortex. *Frontiers in Neuroanatomy*, *15*. https://doi.org/10.3389/fnana.2021.712862

Cachia, A., Borst, G., Tissier, C., Fisher, C., Plaze, M., Gay, O., Rivière, D., Gogtay, N., Giedd, J., Mangin, J.-F., Houdé, O., & Raznahan, A. (2016). Longitudinal stability of the folding pattern of the anterior cingulate cortex during development. *Developmental Cognitive Neuroscience*, *19*, 122–127. https://doi.org/10.1016/j.dcn.2016.02.011

Cachia, A., Borst, G., Vidal, J., Fischer, C., Pineau, A., Mangin, J.-F., & Houdé, O. (2014). The Shape of the ACC Contributes to Cognitive Control Efficiency in Preschoolers. *Journal of Cognitive Neuroscience*, *26*(1), 96–106. https://doi.org/10.1162/jocn_a_00459

Cachia, A., Roell, M., Mangin, J.-F., Sun, Z. Y., Jobert, A., Braga, L., Houde, O., Dehaene, S., & Borst, G. (2018). How interindividual differences in brain anatomy shape reading accuracy. *Brain Structure and Function*, *223*(2), 701–712. https://doi.org/10.1007/s00429-017-1516-x

Chavoshnejad, P., Li, X., Zhang, S., Dai, W., Vasung, L., Liu, T., Zhang, T., Wang, X., & Razavi, M. J. (2021). Role of axonal fibers in the cortical folding patterns: A tale of variability and regularity. *Brain Multiphysics*, *2*, 100029. https://doi.org/10.1016/j.brain.2021.100029

Chi, J. G., Dooling, E. C., & Gilles, F. H. (1977). Gyral development of the human brain. *Annals of Neurology*, *1*(1), 86–93. https://doi.org/10.1002/ana.410010109

Cohen, L., Dehaene, S., Naccache, L., Lehéricy, S., Dehaene-Lambertz, G., Hénaff, M.-A., & Michel, F. (2000). The visual word form area: Spatial and temporal characterization of an initial stage of

reading in normal subjects and posterior split-brain patients. *Brain*, *123*(2), 291–307. https://doi.org/10.1093/brain/123.2.291

Dale, A. M., Fischl, B., & Sereno, M. I. (1999). Cortical Surface-Based Analysis. *NeuroImage*, *9*(2), 179–194. https://doi.org/10.1006/nimg.1998.0395

Dannhoff, G., Poudel, P. P., Bhattarai, C., Kalthur, S. G., & Maldonado, I. L. (2023). Depicting the anatomy of the gyral white matter: Ubi sumus? quo vadimus? *Brain Communications*, *5*(5), fcad265. https://doi.org/10.1093/braincomms/fcad265

Dehaene, S., & Cohen, L. (2007). Cultural Recycling of Cortical Maps. *Neuron*, *56*(2), 384–398. https://doi.org/10.1016/j.neuron.2007.10.004

Dehaene, S., & Cohen, L. (2011). The unique role of the visual word form area in reading. *Trends in Cognitive Sciences*, *15*(6), 254–262. https://doi.org/10.1016/j.tics.2011.04.003

Dehaene, S., Cohen, L., Morais, J., & Kolinsky, R. (2015). Illiterate to literate: Behavioural and cerebral changes induced by reading acquisition. *Nature Reviews Neuroscience*, *16*(4), 234–244. https://doi.org/10.1038/nrn3924

Dehaene-Lambertz, G., Monzalvo, K., & Dehaene, S. (2018). The emergence of the visual word form: Longitudinal evolution of category-specific ventral visual areas during reading acquisition. In *PLoS Biology* (Vol. 16, Issue 3). https://doi.org/10.1371/journal.pbio.2004103

Dubois, J., Benders, M., Borradori-Tolsa, C., Cachia, A., Lazeyras, F., Ha-Vinh Leuchter, R., Sizonenko, S. V., Warfield, S. K., Mangin, J. F., & Hüppi, P. S. (2008). Primary cortical folding in the human newborn: An early marker of later functional development. *Brain*, *131*(8), 2028–2041. https://doi.org/10.1093/brain/awn137

Dubois, J., Dehaene-Lambertz, G., Kulikova, S., Poupon, C., Hüppi, P. S., & Hertz-Pannier, L. (2014). The early development of brain white matter: A review of imaging studies in fetuses, newborns and infants. *Neuroscience*, *276*, 48–71. https://doi.org/10.1016/j.neuroscience.2013.12.044

Dubois, J., Lefèvre, J., Angleys, H., Leroy, F., Fischer, C., Lebenberg, J., Dehaene-Lambertz, G., Borradori-Tolsa, C., Lazeyras, F., Hertz-Pannier, L., Mangin, J.-F., Hüppi, P. S., & Germanaud, D. (2019). The dynamics of cortical folding waves and prematurity-related deviations revealed by spatial and spectral analysis of gyrification. *NeuroImage*, *185*, 934–946. https://doi.org/10.1016/j.neuroimage.2018.03.005

Dunn, L. M., & Dunn, D. M. (2007). *Peabody Picture Vocabulary Test—Fourth Edition*. Minneapolis, MN: Pearson. https://doi.org/10.1037/t15144-000

Fehlbaum, L. V., Peters, L., Dimanova, P., Roell, M., Borbás, R., Ansari, D., & Raschle, N. M. (2022). Mother-child similarity in brain morphology: A comparison of structural characteristics of the brain's reading network. *Developmental Cognitive Neuroscience*, *53*, 101058. https://doi.org/10.1016/j.dcn.2022.101058

Feldt, L. S., Woodruff, D. J., & Salih, F. A. (1987). Statistical Inference for Coefficient Alpha. *Applied Psychological Measurement*, *11*(1), 93–103. https://doi.org/10.1177/014662168701100107

Fischl, B., Sereno, M. I., & Dale, A. M. (1999). Cortical Surface-Based Analysis: II: Inflation, Flattening, and a Surface-Based Coordinate System. *NeuroImage*, *9*(2), 195–207. https://doi.org/10.1006/nimg.1998.0396

Fukutomi, H., Glasser, M. F., Murata, K., Akasaka, T., Fujimoto, K., Yamamoto, T., Autio, J. A., Okada, T., Togashi, K., Zhang, H., Van Essen, D. C., & Hayashi, T. (2019). Diffusion Tensor Model links to Neurite Orientation Dispersion and Density Imaging at high b-value in Cerebral Cortical Gray Matter. *Scientific Reports*, *9*(1), 12246. https://doi.org/10.1038/s41598-019-48671-7

Gaillard, R., Naccache, L., Pinel, P., Clémenceau, S., Volle, E., Hasboun, D., Dupont, S., Baulac, M., Dehaene, S., Adam, C., & Cohen, L. (2006). Direct Intracranial, fMRI, and Lesion Evidence for the Causal Role of Left Inferotemporal Cortex in Reading. *Neuron*, *50*(2), 191–204. https://doi.org/10.1016/j.neuron.2006.03.031

Garel, C., Chantrel, E., Brisse, H., Elmaleh, M., Luton, D., Oury, J.-F., Sebag, G., & Hassan, M. (2001). Fetal Cerebral Cortex: Normal Gestational Landmarks Identified Using Prenatal MR Imaging. *American Journal of Neuroradiology*, *22*(1), 184–189.

Garrison, J. R., Fernyhough, C., McCarthy-Jones, S., Haggard, M., & Simons, J. S. (2015). Paracingulate sulcus morphology is associated with hallucinations in the human brain. *Nature Communications*, *6*(1), Article 1. https://doi.org/10.1038/ncomms9956

Ge, F., Li, X., Razavi, M. J., Chen, H., Zhang, T., Zhang, S., Guo, L., Hu, X., Wang, X., & Liu, T. (2018). Denser Growing Fiber Connections Induce 3-hinge Gyral Folding. *Cerebral Cortex (New York, N.Y.: 1991)*, *28*(3), 1064–1075. https://doi.org/10.1093/cercor/bhx227

Gratiolet, P. (1854). *Mémoire sur les plis cérébraux de l'homme et des primates* (Vol. 1). A. Bertrand. https://books.google.com/books?hl=fr&lr=&id=JiNCAAAAcAAJ&oi=fnd&pg=PA1&dq=Gratiole t+LP+(1854)+M%C3%A9moire+sur+les+plis+c%C3%A9r%C3%A9braux+de+l%E2%80%99 homme+et+des+primates&ots=s15dgI7NeU&sig=e5cwl2zAb_NaucmQjbysfY2Gf2s

Gratton, C., Nelson, S. M., & Gordon, E. M. (2022). Brain-behavior correlations: Two paths toward reliability. *Neuron*, *110*(9), 1446–1449. https://doi.org/10.1016/j.neuron.2022.04.018

Grill-Spector, K., & Weiner, K. S. (2014). The functional architecture of the ventral temporal cortex and its role in categorization. *Nature Reviews Neuroscience*, *15*(8), 536–548. https://doi.org/10.1038/nrn3747

Grotheer, M., Yeatman, J., & Grill-Spector, K. (2021). White matter fascicles and cortical microstructure predict reading-related responses in human ventral temporal cortex. *NeuroImage*, *227*(August 2020), 117669. https://doi.org/10.1016/j.neuroimage.2020.117669

Hansen, P. E., Ballesteros, M. C., Soila, K., Garcia, L., & Howard, J. M. (1993). MR imaging of the developing human brain. Part 1. Prenatal development. *RadioGraphics*, *13*(1), 21–36. https://doi.org/10.1148/radiographics.13.1.8426929

Hosseini, S. M. H., Black, J. M., Soriano, T., Bugescu, N., Martinez, R., Raman, M. M., Kesler, S. R., & Hoeft, F. (2013). Topological properties of large-scale structural brain networks in children with familial risk for reading difficulties. *NeuroImage*, *71*, 260–274. https://doi.org/10.1016/j.neuroimage.2013.01.013

Huntgeburth, S. C., & Petrides, M. (2012). Morphological patterns of the collateral sulcus in the human brain. *European Journal of Neuroscience*, *35*(8), 1295–1311. https://doi.org/10.1111/j.1460-9568.2012.08031.x

Im, K., Raschle, N. M., Smith, S. A., Ellen Grant, P., & Gaab, N. (2016). Atypical Sulcal Pattern in Children with Developmental Dyslexia and At-Risk Kindergarteners. *Cerebral Cortex*, *26*(3), 1138–1148. https://doi.org/10.1093/cercor/bhu305

Kubota, E., Grill-Spector, K., & Nordt, M. (2023). Rethinking cortical recycling in ventral temporal cortex. *Trends in Cognitive Sciences*, 1–10. https://doi.org/10.1016/j.tics.2023.09.006

Lahutsina, A., Spaniel, F., Mrzilkova, J., Morozova, A., Brabec, M., Musil, V., & Zach, P. (2023). Morphology of Anterior Cingulate Cortex and Its Relation to Schizophrenia. *Journal of Clinical Medicine*, *12*(1), Article 1. https://doi.org/10.3390/jcm12010033

Lazari, A., & Lipp, I. (2021). Can MRI measure myelin? Systematic review, qualitative assessment, and meta-analysis of studies validating microstructural imaging with myelin histology. *NeuroImage*, *230*(January), 117744. https://doi.org/10.1016/j.neuroimage.2021.117744

Lefly, D. L., & Pennington, B. F. (2000). Reliability and validity of the adult reading history questionnaire. *Journal of Learning Disabilities*. https://doi.org/10.1177/002221940003300306

Li, J., Osher, D. E., Hansen, H. A., & Saygin, Z. M. (2020). Innate connectivity patterns drive the development of the visual word form area. *Scientific Reports*, *10*(1), 1–13. https://doi.org/10.1038/s41598-020-75015-7

Lyu, I., Bao, S., Hao, L., Yao, J., Miller, J. A., Voorhies, W., Taylor, W. D., Bunge, S. A., Weiner, K. S., & Landman, B. A. (2021). Labeling lateral prefrontal sulci using spherical data augmentation and context-aware training. *NeuroImage*, *229*, 117758. https://doi.org/10.1016/j.neuroimage.2021.117758

Maboudian, S. A., Willbrand, E. H., Kelly, J. P., Jagust, W. J., Weiner, K. S., & Initiative, for the A. D. N. (2024). Defining Overlooked Structures Reveals New Associations between the Cortex and Cognition in Aging and Alzheimer's Disease. *Journal of Neuroscience*, *44*(16). https://doi.org/10.1523/JNEUROSCI.1714-23.2024

Madan, C. R. (2019). Robust estimation of sulcal morphology. *Brain Informatics*, *6*(1), 1–11. https://doi.org/10.1186/s40708-019-0098-1

Mangin, J.-F., Le Guen, Y., Labra, N., Grigis, A., Frouin, V., Guevara, M., Fischer, C., Rivière, D., Hopkins, W. D., Régis, J., & Sun, Z. Y. (2019). "Plis de passage" Deserve a Role in Models of the Cortical Folding Process. *Brain Topography*, *32*(6), 1035–1048. https://doi.org/10.1007/s10548-019-00734-8

McGrew, K. S., & Schrank, F. A. (2007). Woodcock-Johnson III normative update—Technical manual. *Rolling Meadows, IL: Riverside*.

Miller, J. A., Voorhies, W. I., Lurie, D. J., D'Esposito, M., & Weiner, K. S. (2021). Overlooked tertiary sulci serve as a meso-scale link between microstructural and functional properties of human lateral prefrontal cortex. *Journal of Neuroscience*, *41*(10), 2229–2244. https://doi.org/10.1523/JNEUROSCI.2362-20.2021

Moulton, E., Bouhali, F., Monzalvo, K., Poupon, C., Zhang, H., Dehaene, S., Dehaene-Lambertz, G., & Dubois, J. (2019). Connectivity between the visual word form area and the parietal lobe improves after the first year of reading instruction: A longitudinal MRI study in children. *Brain Structure and Function*, 1–18. https://doi.org/10.1007/s00429-019-01855-3

Myers, C. A., Vandermosten, M., Farris, E. A., Hancock, R., Gimenez, P., Black, J. M., Casto, B., Drahos, M., Tumber, M., Hendren, R. L., Hulme, C., & Hoeft, F. (2014). White Matter Morphometric Changes Uniquely Predict Children's Reading Acquisition. *Psychological Science*, *25*(10), 1870–1883. https://doi.org/10.1177/0956797614544511

Natu, V. S., Arcaro, M. J., Barnett, M. A., Gomez, J., Livingstone, M., Grill-Spector, K., & Weiner, K. S. (2021). Sulcal Depth in the Medial Ventral Temporal Cortex Predicts the Location of a Place-Selective Region in Macaques, Children, and Adults. *Cerebral Cortex*, *31*(1), 48–61. https://doi.org/10.1093/cercor/bhaa203

Papini, C., Palaniyappan, L., Kroll, J., Froudist-Walsh, S., Murray, R. M., & Nosarti, C. (2020). Altered Cortical Gyrification in Adults Who Were Born Very Preterm and Its Associations With Cognition and Mental Health. *Biological Psychiatry: Cognitive Neuroscience and Neuroimaging*, *5*(7), 640–650. https://doi.org/10.1016/j.bpsc.2020.01.006

Parker, B. J., Voorhies, W. I., Jiahui, G., Miller, J. A., Willbrand, E., Hallock, T., Furl, N., Garrido, L., Duchaine, B., & Weiner, K. S. (2023). Hominoid-specific sulcal variability is related to face perception ability. *Brain Structure and Function*, *228*(2), 677–685. https://doi.org/10.1007/s00429-023-02611-4

Pillet, I., Cerrahoğlu, B., Philips, R. V., Dumoulin, S., & de Beeck, H. O. (2024). The position of visual word forms in the anatomical and representational space of visual categories in occipitotemporal cortex. *Imaging Neuroscience*, *2*, 1–28. https://doi.org/10.1162/imag_a_00196

Reuter, M., Schmansky, N. J., Rosas, H. D., & Fischl, B. (2012). Within-subject template estimation for unbiased longitudinal image analysis. *NeuroImage*, *61*(4), 1402–1418. https://doi.org/10.1016/J.NEUROIMAGE.2012.02.084

Reveley, C., Seth, A. K., Pierpaoli, C., Silva, A. C., Yu, D., Saunders, R. C., Leopold, D. A., & Ye, F. Q. (2015). Superficial white matter fiber systems impede detection of long-range cortical connections in diffusion MR tractography. *Proceedings of the National Academy of Sciences of the United States of America*, *112*(21), E2820–E2828. https://doi.org/10.1073/pnas.1418198112

Rivière, D., Leprince, Y., Labra, N., Vindas, N., Foubet, O., Cagna, B., Loh, K. K., Hopkins, W., Balzeau, A., Mancip, M., Lebenberg, J., Cointepas, Y., Coulon, O., & Mangin, J.-F. (2022). Browsing Multiple Subjects When the Atlas Adaptation Cannot Be Achieved via a Warping Strategy. *Frontiers in Neuroinformatics*, *16*, 803934. https://doi.org/10.3389/fninf.2022.803934

Roell, M., Cachia, A., Matejko, A. A., Houdé, O., Ansari, D., & Borst, G. (2021). Sulcation of the intraparietal sulcus is related to symbolic but not non-symbolic number skills. *Developmental Cognitive Neuroscience*, *51*, 100998. https://doi.org/10.1016/j.dcn.2021.100998

Rosenberg, M. D., & Finn, E. S. (2022). How to establish robust brain–behavior relationships without thousands of individuals. *Nature Neuroscience*, 0–2. https://doi.org/10.1038/s41593-022-01110-9

Rosseel, Y. (2012). lavaan: An R Package for Structural Equation Modeling. *Journal of Statistical Software*, *48*(2). https://doi.org/10.18637/jss.v048.i02

Santacroce, F., Cachia, A., Fragueiro, A., Grande, E., Roell, M., Baldassarre, A., Sestieri, C., & Committeri, G. (2024). Human intraparietal sulcal morphology relates to individual differences in language and memory performance. *Communications Biology*, *7*(1), 1–8. https://doi.org/10.1038/s42003-024-06175-9

Saygin, Z. M., Osher, D. E., Norton, E. S., Youssoufian, D. A., Beach, S. D., Feather, J., Gaab, N., Gabrieli, J. D. E. E., & Kanwisher, N. (2016). Connectivity precedes function in the development of the visual word form area. *Nature Neuroscience*, *19*(9), 1250–1255. https://doi.org/10.1038/nn.4354

Schilling, K. G., Blaber, J., Hansen, C., Cai, L., Rogers, B., Anderson, A. W., Smith, S., Kanakaraj, P., Rex, T., Resnick, S. M., Shafer, A. T., Cutting, L. E., Woodward, N., Zald, D., & Landman, B. A. (2020). Distortion correction of diffusion weighted MRI without reverse phase-encoding scans or field-maps. *PLoS ONE*, *15*(7 July), 1–15. https://doi.org/10.1371/journal.pone.0236418

Schmitt, S., Ringwald, K. G., Meller, T., Stein, F., Brosch, K., Pfarr, J.-K., Hahn, T., Lemke, H., Meinert, S., Repple, J., Thiel, K., Waltemate, L., Winter, A., Grotegerd, D., Dempfle, A., Jansen, A., Krug, A., Dannlowski, U., Nenadić, I., & Kircher, T. (2023). Associations of gestational age with gyrification and neurocognition in healthy adults. *European Archives of Psychiatry and Clinical Neuroscience*, *273*(2), 467–479. https://doi.org/10.1007/s00406-022-01454-0

Schwizer Ashkenazi, S., Roell, M., McCaskey, U., Cachia, A., Borst, G., O'Gorman Tuura, R., & Kucian, K. (2024). Are numerical abilities determined at early age? A brain morphology study in children and adolescents with and without developmental dyscalculia. *Developmental Cognitive Neuroscience*, *67*, 101369. https://doi.org/10.1016/j.dcn.2024.101369

Shinohara, H., Liu, X., Nakajima, R., Kinoshita, M., Ozaki, N., Hori, O., & Nakada, M. (2020). Pyramid-shape crossings and intercrossing fibers are key elements for construction of the neural network in the superficial white matter of the human cerebrum. *Cerebral Cortex*, *30*(10), 5218–5228. https://doi.org/10.1093/cercor/bhaa080

Skeide, M. A., Kraft, I., Müller, B., Schaadt, G., Neef, N. E., Brauer, J., Wilcke, A., Kirsten, H., Boltze, J., & Friederici, A. D. (2016). NRSN1 associated grey matter volume of the visual word form area reveals dyslexia before school. *Brain*, *139*(10), 2792–2803. https://doi.org/10.1093/brain/aww153

Tissier, C., Linzarini, A., Allaire-Duquette, G., Mevel, K., Poirel, N., Dollfus, S., Etard, O., Orliac, F., Peyrin, C., Charron, S., Raznahan, A., Houdé, O., Borst, G., & Cachia, A. (2018). Sulcal polymorphisms of the IFC and ACC contribute to inhibitory control variability in children and

adults. *eNeuro*, *5*(1). https://doi.org/10.1523/ENEURO.0197-17.2018

Torgesen, J. K., Wagner, R. K., & Rashotte, C. A. (1999). TOWRE: Test of word reading reading efficiency. *The Psychological Corporation*.

Vandermosten, M., Hoeft, F., & Norton, E. S. (2016). Integrating MRI brain imaging studies of pre-reading children with current theories of developmental dyslexia: A review and quantitative meta-analysis. *Current Opinion in Behavioral Sciences*, *10*(June), 155–161. https://doi.org/10.1016/j.cobeha.2016.06.007

Vandermosten, M., Schevenels, K., Economou, M., & Hoeft, F. (2020). The influence of intergenerational transfer of white matter tracts on early reading development. *bioRxiv*, 2020.10.09.333096.

Veraart, J., Novikov, D. S., Christiaens, D., Ades-aron, B., Sijbers, J., & Fieremans, E. (2016). Denoising of diffusion MRI using random matrix theory. *NeuroImage*, *142*, 394–406. https://doi.org/10.1016/j.neuroimage.2016.08.016

Voorhies, W. I., Miller, J. A., Yao, J. K., Bunge, S. A., & Weiner, K. S. (2021). Cognitive insights from tertiary sulci in prefrontal cortex. *Nature Communications*, *12*(1), 1–14. https://doi.org/10.1038/s41467-021-25162-w

Wagner, R., Torgesen, J., Rashotte, C., & Pearson, N. (1999). *Comprehensive test of phonological processing: CTOPP*.

Weiner, K. S. (2019). The Mid-Fusiform Sulcus (sulcus sagittalis gyri fusiformis). *Anatomical Record*, *302*(9), 1491–1503. https://doi.org/10.1002/ar.24041

Weiner, K. S. (2023). The hypothesis of fundal cognition. *Nature Reviews Neuroscience*, *24*(9), 521–521. https://doi.org/10.1038/s41583-023-00725-6

Weiner, K. S., Golarai, G., Caspers, J., Chuapoco, M. R., Mohlberg, H., Zilles, K., Amunts, K., & Grill-Spector, K. (2014). The mid-fusiform sulcus: A landmark identifying both cytoarchitectonic and functional divisions of human ventral temporal cortex. *NeuroImage*, *84*, 453–465. https://doi.org/10.1016/j.neuroimage.2013.08.068

Weiner, K. S., Yeatman, J. D., & Wandell, B. A. (2017). The posterior arcuate fasciculus and the vertical occipital fasciculus. *Cortex*, *97*, 274–276. https://doi.org/10.1016/j.cortex.2016.03.012

Wickham, H. (2016). *ggplot2: Elegant Graphics for Data Analysis*. Springer-Verlag New York. https://ggplot2.tidyverse.org

Willbrand, E. H., Voorhies, W. I., Yao, J. K., Weiner, K. S., & Bunge, S. A. (2022). Presence or absence of a prefrontal sulcus is linked to reasoning performance during child development. *Brain Structure and Function*, *227*(7), 2543–2551. https://doi.org/10.1007/s00429-022-02539-1

Wilson, S. M., Rising, K., Stib, M. T., Rapcsak, S. Z., & Beeson, P. M. (2013). Dysfunctional visual word form processing in progressive alexia. *Brain*, *136*(4), 1260–1273. https://doi.org/10.1093/brain/awt034

Winkler, A. M., Ridgway, G. R., Webster, M. A., Smith, S. M., & Nichols, T. E. (2014). Permutation inference for the general linear model. *NeuroImage*, *92*, 381–397. https://doi.org/10.1016/j.neuroimage.2014.01.060

Wolf, M., & Denckla, M. (2005). *RAN/RAS: Rapid automatized naming and rapid alternating stimulus tests*. https://www.proedinc.com/Products/10435/ranras-rapid-automatized-naming-and-rapid-altern.aspx

Woodcock, R. W. (1998). *Woodcock Reading Mastery Tests-Revised Normative Update: Examiner's manual*. Circle Pines, MN: American Guidance Service.

Woolnough, O., & Tandon, N. (2024). Dissociation of reading and naming in ventral occipitotemporal cortex. *Brain*, *147*(7), 2522–2529. https://doi.org/10.1093/brain/awae027

Xia, Z., Wang, C., Hancock, R., Vandermosten, M., & Hoeft, F. (2021). Development of thalamus mediates paternal age effect on offspring reading: A preliminary investigation. *Human Brain Mapping*, *42*(14), 4580–4596. https://doi.org/10.1002/hbm.25567

Yamagata, B., Murayama, K., Black, J. M., Hancock, R., Mimura, M., Yang, T. T., Reiss, A. L., & Hoeft, F. (2016). Female-specific intergenerational transmission patterns of the human corticolimbic circuitry. *Journal of Neuroscience*, *36*(4), 1254–1260. https://doi.org/10.1523/JNEUROSCI.4974-14.2016

Yao, J. K., Voorhies, W. I., Miller, J. A., Bunge, S. A., & Weiner, K. S. (2022). Sulcal depth in prefrontal cortex: A novel predictor of working memory performance. *Cerebral Cortex*. https://doi.org/10.1093/cercor/bhac173

Yeatman, J. D., Dougherty, R. F., Ben-Shachar, M., & Wandell, B. A. (2012). Development of white matter and reading skills. *Proceedings of the National Academy of Sciences*, *109*(44), E3045–E3053. https://doi.org/10.1073/pnas.1206792109

Zaretskaya, N., Fischl, B., Reuter, M., Renvall, V., & Polimeni, J. R. (2018). Advantages of cortical surface reconstruction using submillimeter 7 T MEMPRAGE. *NeuroImage*, *165*(June 2017), 11–26. https://doi.org/10.1016/j.neuroimage.2017.09.060

Zemmoura, I., Herbet, G., Moritz-Gasser, S., & Duffau, H. (2015). New insights into the neural network mediating reading processes provided by cortico-subcortical electrical mapping. *Human Brain*

*Mapping*, *36*(6), 2215–2230. https://doi.org/10.1002/hbm.22766

Zhan, M., Pallier, C., Agrawal, A., Dehaene, S., & Cohen, L. (2023). Does the visual word form area split in bilingual readers? A millimeter-scale 7-T fMRI study. *Science Advances*, *9*(14), eadf6140. https://doi.org/10.1126/sciadv.adf6140

Zhang, T., Li, X., Jiang, X., Ge, F., Zhang, S., Zhao, L., Liu, H., Huang, Y., Wang, X., Yang, J., Guo, L., Hu, X., & Liu, T. (2020). Cortical 3-hinges could serve as hubs in cortico-cortical connective network. *Brain Imaging and Behavior*, *14*(6), 2512–2529. https://doi.org/10.1007/s11682-019-00204-6